CHALMERS

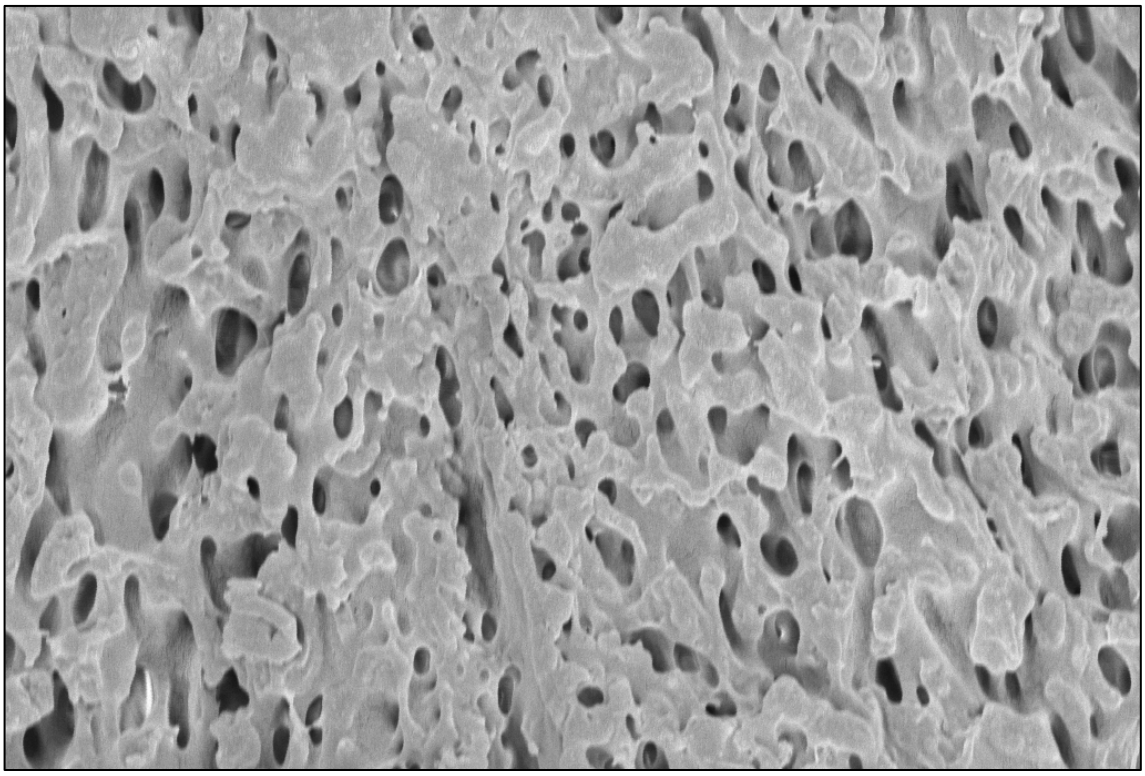

Molecular weight dependence of polymer leaching and mass transport through ethyl cellulose/hydroxypropyl cellulose films

Master of Science Thesis

SOFIE OLSSON

Department of Chemical and Biological Engineering
Division of Applied Chemistry
CHALMERS UNIVERSITY OF TECHNOLOGY
Gothenburg, Sweden, 2011
Report No. 403

REPORT NO. 403

Molecular weight dependence of polymer leaching and mass transport through ethyl cellulose/hydroxypropyl cellulose films

SOFIE OLSSON

SUPERVISOR:
Helene Andersson, SIK - The Swedish Institute for Food and Biotechnology

EXAMINER:
Annette Larsson, Chalmers University of Technology

Department of Chemical and Biological Engineering
Division of Applied Chemistry
CHALMERS UNIVERSITY OF TECHNOLOGY
Göteborg, Sweden 2012

Molecular weight dependence of polymer leaching and mass transport through ethyl cellulose/hydroxypropyl cellulose films

SOFIE OLSSON

Technical report no 403
Department of Chemical and Biological Engineering
Division of Applied Chemistry
Chalmers University of Technology
SE-412 96 Göteborg
Sweden
Telephone + 46 (0)31-772 1000

Chalmers University of Technology
Göteborg, Sweden 2012

Molecular weight dependence of polymer leaching and mass transport through ethyl cellulose/hydroxypropyl cellulose films

SOFIE OLSSON
Department of Chemical and Biological Engineering
Division of Applied Chemistry
Chalmers University of Technology

ABSTRACT

Controlled release is an important concept in the pharmaceutical industry, with the goal to deliver a drug to the right place, at the right time and in sufficient amounts. There are many different approaches to controlled release systems, and one of these is using porous polymer coatings surrounding the active substance. By controlling the development, size and shape of the pores, the rate of administration can be optimized to match the application.

Porous polymer coatings can be composed of water-insoluble ethyl cellulose (EC) together with water-soluble hydroxypropyl cellulose (HPC). EC/HPC solutions phase separate upon solvent evaporation and this happens during the manufacture of the coating. Previous studies have shown that using a minor amount of HPC (30%) and a major amount of EC creates films with an interconnected network of HPC in the EC matrix. The HPC will, when exposed to water, leach out from the film leaving a porous network where the drug can diffuse out. This is important since the non-porous coating is originally impermeable to the drug.

In this study the dependence of molecular weight of HPC on the pore formation was investigated by measuring the permeability of films containing different molecular weight HPC. Also the amount of HPC that leached out from these films was measured. The investigation was performed using side-by-side diffusion cells and mass transfer through the film was measured by using radioactively labelled markers. The amount of leached HPC was measured using size exclusion chromatography together with a refractive index detector. In addition the internal structures of the films were investigated using scanning electron microscopy.

The results showed that the permeability and HPC leaching was very dependent on the molecular weight of HPC, with permeability increasing from low to medium molecular weight and then decreasing for the highest molecular weight HPC. This implies the existence of a maximum for the film permeability, which would make it possible to fine-tune the permeability and porous structure to fit the application by selecting the optimal molecular weight HPC.

Keywords: Hydroxypropyl cellulose, ethyl cellulose, molecular weight, permeability, pharmaceutical coating, phase separation, polymer leaching, porous coating, controlled release, internal structure

Table of contents

1 Introduction

Inventing new drugs and designing new formulations to treat diseases in a better and more efficient way is an important aim of the pharmaceutical industry. A more efficient treatment could mean i.e. by cheaper means, without as many complications for the patient, and by more efficient or more convenient routes of administration.

The efficacy of a pharmaceutical substance is determined not only by the chemical substance itself but also the concentration of the active substance at the specific target site in the human body. Too low concentrations yields no or too low effect and too high concentrations increase the risk of side effects and toxicity. Due to this a major aspiration of the pharmaceutical industry is to deliver the drug to the right place, at the right time and in sufficient amounts. This concept is known as controlled release. There are different approaches to controlled release systems, such as designing the actual drug for modified release, integrating the drug into a gel matrix that dissolves in the body or by the use of different coatings surrounding the active substance [1].

Coatings made out of a variety of polymers can be used for oral controlled release formulations by allowing a slow transport across the material and, thus, prolonging the therapeutic concentration in the blood. By combining various polymers different properties of the coatings can be achieved. One such polymer combination is the use of the water-insoluble ethyl cellulose (EC) together with the water-soluble hydroxypropyl cellulose (HPC). Both EC and HPC are easily made into films and have low toxicity [2], which makes them suitable for use as pellet coatings in the pharmaceutical industry and also for other non-pharmaceutical applications.

1.1.1 EC/HPC coatings

EC and HPC are not compatible unless dissolved in diluted amounts in a common solvent. When the solvent evaporates the polymer solution undergoes a phase separation and different domains rich in each polymer is created. This is taken advantage of when creating films out of EC and HPC and the result is films with volumes of the water soluble HPC in a matrix of EC or the opposite. If the two polymers are combined in specific amounts the volumes of HPC can interconnect and form a continuous network of HPC in the EC matrix [2]. This is especially interesting for controlled release applications, as this will yield a porous film coating when subjected to water. Pure EC films are generally semi-permeable, which means that while water can pass through the intact film the larger active substances cannot. In order to control the administration of the drug it can therefore be of interest to study these porous systems.

When a film like that is immersed in water the water will begin to penetrate the film, which will lead to dissolution of HPC, beginning at the surface of the film and continuing in the bulk as the water penetrates the HPC rich domains. Once HPC has dissolved it will start to diffuse and will eventually leach out from the film and thereby creating empty voids, which will ease the water penetration and open up new areas of the film. These empty voids form pores in the film and, if interconnected, will allow for mass transport across the film. With the porous network being formed the active substance enclosed by the film coating can be dissolved by water reaching the core. The active substance then leach out of the pellet by diffusion through the porous network, i.e. a therapeutic level of the drug can be held constant in the body for a prolonged period of time since the active substance is released with a defined rate.

The formation of a porous network depends on the phase separation of the two polymers and the fraction of HPC in the coating, because in order for pore formation to occur there has to be a continuous network of HPC in the EC phase. The formation of a continuous network is

dependent on the amount of HPC available and the shape of the HPC phases. Marucci et al have shown that the films demonstrate a drastic increase in permeability at a critical HPC concentration, which can be explained using a percolation theory [2]. The percolation theory describes the formation of a more continuous phase of HPC with a joint network of HPC volumes in the film, hence less HPC is "trapped" within the EC phase. Films with 30% w/w HPC was shown to become permeable with HPC leaching [2] and SEM images of such films revealed a complex and highly porous internal structure [3].

The initial lag time before diffusion over the film can occur has been shown to be dependent on both the amount of HPC in the film [2] and the thickness of the film [4]. The lag time was shown to exhibit a non-linear dependence on film thickness, which corresponds with the lower leaching rates from thicker films that was also discovered [4], and high amount of HPC in the films showed shorter lag times than low amounts [2].

Andersson et al have shown the molecular weight of the EC to be important for the pore morphology, total HPC leaching and permeability of EC/HPC mixed films [3], but no investigation regarding molecular weight of HPC for the same factors has been performed. Nor has the leaching rate of HPC and the pore morphological contribution on HPC leaching been investigated thoroughly for these films.

1.2 Objective

The aim was to study how the leaching of HPC depends on the molecular weight of HPC and if there were any differences between the two sides of the film regarding the amount of leached polymer. The permeability of the film and how this was affected by the molecular weight of HPC together with the impact on lag-times, i.e. the time before the film is fully permeable, was investigated. Also, the relation between the leaching rate and the change of permeability over time was studied together with a comprehensive investigation of the internal structure of the different EC/HPC mixed films.

2 Theoretical background

2.1 Cellulose ethers

With today's great interest in finding renewable sources for polymeric materials, cellulose, being one of the most commonly occurring polymers in nature [5], is an interesting research topic. Cellulose is a carbohydrate with the general formula shown in Figure 1. In the natural occurring non-modified cellulose the R denoted in Figure 1 is hydrogen, which together with the oxygen atoms form strong hydrogen bonds between the polymer chains. The properties of the polymer can, however, be altered by replacing the hydrogen with other atoms or molecules, e.g. to form cellulose ethers. For example the solubility of the modified cellulose ether is dependent on the nature of the substitution ether group, the relation between ether groups and free hydroxyl groups along the polymer chain (degree of substitution), the length of the polymer chain and the uniformity of the single chains regarding substitution and length [5].

Ethyl cellulose and hydroxypropyl cellulose are prepared by replacing the hydrogen with an ethyl ether group and a hydroxypropyl ether group respectively (as shown in Figure 1).

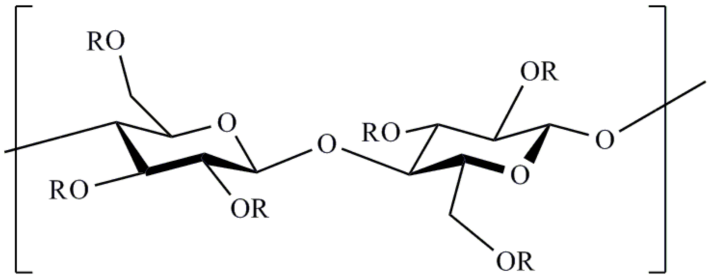

Figure 1: Chemical structure of ethyl cellulose and hydroxypropyl cellulose. In ethyl cellulose R= H or CH_2CH_3, in hydroxypropyl cellulose R = H or $CH_2CH(OH)CH_3$ and in unmodified cellulose R = H

The number of substituted hydroxyl groups is referred to as degree of substitution and is important for the properties of the polymers [6]. HPC can be substituted to a higher extent than the three "original" hydroxyl groups since the substitution molecule also contains a hydroxyl group that can be substituted in a similar manner. The water solubility of HPC derives from this substitution, as cellulose itself is insoluble. The water solubility of the modified cellulose is not due to the addition of a hydrophilic group, since the hydroxyl group that was substituted is much more hydrophilic than the substitution group. The solubility rather stems from the fact that the long substitution groups increase the distance between the chains by sterical hindrance and thereby breaks the strong bonds between them [7].

2.2 Phase separation of polymer mixtures

Creating a polymer solution can be difficult as these solutions often undergo a phase separation instead of proper mixing. This difficulty arises from the low entropy of a polymer compared to the single monomers or solvent molecules. By visualizing the polymer as a string of smaller molecules (monomers) bound together the reduction in entropy of this molecule becomes clear (Flory-Huggins theory) as the system is clearly less disordered. The entropy always acts in favour of mixing and therefore has a large impact on whether a polymer will dissolve or not [8]. The enthalpy, however, can act both in favour of and against mixing, depending on the intermolecular forces etc. within the system, and due to this polymers can be soluble even though having a low entropy of mixing [8].

Mixtures of two polymers and a solvent, ternary mixtures, are often two-phase systems with individual phases rich in each polymer. These two individual phases originate from polymer incompatibility where the polymers are not miscible with each other. By the addition of a common solvent these counteracting driving forces can be diminished and a polymer solution is formed for low polymer concentrations [9].

Phase separation can occur by two different mechanisms, nucleation and growth and spinodal decomposition. Which of these two that will occur depends on the concentrations of the polymers and the solvent, that is, it depends on where in the phase diagram the system is. A phase diagram is dependent on the system and therefore needs to be defined for each system. Spinodal decomposition appears uniformly throughout the material while nucleation and growth, as the name implies, occurs by nucleation and is therefore not uniformly occurring throughout the material.

The EC/HPC system has previously been shown to phase separate due to polymer incompatibility [10]. By dissolving the two polymers in the common solvent ethanol the aforementioned polymer-polymer interactions are diluted and it is possible to form EC/HPC solutions. However, as the solvent evaporates and the polymer concentration in the solution increases, phase separation occurs with one polymer dispersed in a matrix of the other polymer or a bicontinuous system depending on the volume fractions of the two polymers.

2.3 Permeability & Diffusion

Permeability, which could be defined as the ability of a material to transport a fluid through itself [11], is an important property for barrier materials of different kinds. A way of measuring the permeability is by using diffusion cells with the material placed between two cells filled with a liquid (e.g. water) and measuring the diffusion from the one cell (donor cell) to the other (receiver cell).

The diffusion through a film can be described by using Fick's first law describing a one-dimensional net flux through the film [12]

$$J = -D\frac{\partial c}{\partial x}$$

where A is the area through which the diffusion occurs, D is the diffusion coefficient, c is the concentration and x is the distance.

The above expression could also be written

$$J = \frac{1}{A}\frac{\partial m}{\partial t}$$

where $\partial m/\partial t$ is the mass transfer rate.

By combining the two expressions above, assuming steady-state conditions and the concentration in the receiver chamber to be zero the following expression is found

$$\frac{1}{A}\frac{\partial m}{\partial t} = D\frac{c_1 - c_2}{x_1 - x_2} = \left\{c_2 \approx 0\right\} = D\frac{c_1}{h}$$

$$\Rightarrow D = \frac{h}{A}\frac{\partial m}{c_1 \partial t}$$

where c_1 is the concentration at the film in the donor chamber, c_2 is the concentration at the film in the receiver chamber (Figure 2) and h is the thickness of the film.

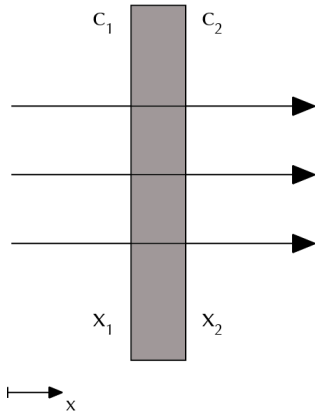

Figure 2: Image describing the diffusion through the film with the concentrations c_1 and c_2 noted and the arrows show the net diffusion.

The permeability of the film is consistent with the diffusion through the film, which yields the following expression for calculating the permeability (if the assumptions mentioned above are still valid)

$$P = D = \frac{h}{A}\frac{\partial m}{\Delta c \partial t}$$

where Δc is the concentration gradient over the film. If $c_1 >> c_2$ then Δc can be approximated by c_1.

Andersson et al have described the permeability of an EC/HPC film to be dependent on the properties of the permeant, the film/pores and the interaction between these [3]. Hence, the permeability can be divided up into these factors forming a new expression [3]

$$P_a = D_{ab} \times C_f \times K_{ra}$$

where D_{ab} is the diffusion coefficient of substance a in medium b, C_f is the film factor and K_{ra} is the hindrance factor.

The hindrance factor describes properties that are due to both the diffusant and the film, such as interactions between the diffusing substance and the pore walls. The film factor describes the properties depending on the film only and is independent of the diffusing substance. And finally the diffusion coefficient describes properties that are solely dependent on the diffusing substance and not on the film. Together these three factors describe the permeability of a film as mentioned.

2.4 Viscosity

The viscosity of a fluid is described as the fluid's resistance to flow, and polymer solutions and melts have higher viscosity than most fluids due to entanglements of the long chains. Newtonian fluids, such as water, have a constant viscosity that does not depend on the rate of the applied stress. Thus, flow behaviour with a viscosity independent of shear rate is usually called Newtonian behaviour. The viscosity of polymer melts and solutions, on the contrary, are shear rate dependent, hence polymers are non-Newtonian fluids and can exhibit behaviours like shear thinning. A polymer melt has a viscosity depending on temperature, molar mass and shear rate. The viscosity of a polymer solution behaves very similar to that of the polymer melt, with two exceptions, it is also concentration dependent and due to the small solvent molecules it is also significantly lower than that of the melt [13].

Viscosity is a very important parameter when it comes to processing of polymers due to the high value, wide range and the dependence on shear rate [14]. Therefore it is important to know the viscosity of the polymer solution.

2.5 Analytical methods

Below are short theoretical descriptions of the analytical methods and equipment used. In short the size exclusion chromatography together with detectors was used for concentration and molecular weight determination. Scanning electron microscopy was used for determination of structural properties of the films and liquid scintillation was used in order to determine the permeability of the film.

2.5.1 Size exclusion chromatography

Chromatography is a two-phase technique based on holding one phase steady (stationary phase) and moving the other phase (mobile phase) past it. The principle is that the different solutes interact differently with the stationary phase and therefore take different amounts of time to pass through [15]. Depending on how the solute interacts with the stationary phase the chromatography could be divided into different categories, such as adsorption-, affinity- and size exclusion chromatography (also named molecular exclusion chromatography, gel filtration etc.) [15].

Size exclusion chromatography (SEC) works like a sieve and separates the molecules according to size by using a porous stationary phase [15]. The smaller solutes can enter the pores of the stationary phase and therefore have a longer pathway through the stationary phase. Consequently, this takes longer time and larger solutes are hence eluted prior to the smaller solutes [13]. By having pores of different sizes in the stationary phase the solutes can be separated into small fractions with the approximately same molecular volume. [13] This technique is often used to separate macromolecules [15], however it is important to remember that the molecules will be separated by volume and not weight, which can differ significantly for macromolecules such as polymers [13].

In polymer chemistry the SEC can be used together with a refractive index detector (RI) and multi-angle light scattering (MALS) to determine molecular weight distribution as well as weight average molecular weight and number average molecular weight of the different fractions without the need to use standards [13]. Due to the ability to determine both the number average molecular weight and the weight average molecular weight of a polymer sample the molecular weight distribution called the polydispersity index (PI) can be calculated. The PI is defined as the weight average molecular weight divided by the number average molecular weight and a monodisperse sample therefore has the PI of one. The SEC together with the RI detector can also be used to determine the concentrations of solutes in a sample.

A refractive index detector measures the difference in refraction between pure solvent and solute in solvent [15], which can be used to calculate the solute concentration. A benefit with using a refractive index detector is its ability to detect almost any solvent regardless of UV light adsorption etc. A drawback is, however, the rather poor sensitivity with the approximate detection limit of 100-1000 ng [16], which makes it impossible to do trace analysis using this detector.

Multi-angle light scattering (MALS) used together with SEC-RI can provide information on absolute molecular weight, conformational information and the size of the molecules. It is possible to determine the radius of gyration (R_G) using MALS, since this technique, unlike low angle light scattering (LALS), measures the angular dependence of the light scattering. This angular dependence is what gives information about the molecular size [17]. Light scattering for water-soluble molecules poses a difficulty since water easily scatter contaminants, which will interfere with the results. To overcome this difficulty filtered mobile phase and a good column support that will not leach out during elution should be used [17]. To avoid degradation of the

samples due to microbial contamination [18] a small amount (0.02%) of NaN_3 can be added to the mobile phase [19].

2.5.2 Scanning electron microscopy

Scanning electron microscopy (SEM) imaging can be used to determine the topographic structure of samples in order to detect differences in e.g. the pore structure of a material. SEM can be used as a conventional microscope for magnification, but also an instrument for determination of the topographic composition of an unknown sample as just mentioned.

The basic principle of SEM is that an electron source emits an electron beam, which sweeps over and interacts with the sample surface. This interaction yields different signals, which gives information on the topography and chemical composition of the sample. The resolution depends on the radius of the electron beam and to improve the resolution magnetic lenses are used to focus the beam. The resolution of a SEM is approximately 5 nm compared to regular optic microscopy, that has a resolution of approximately 500 nm, due to the shorter wavelengths of electrons compared to photons [20]. In order to be examined by SEM the sample has to have a conductive surface, which could derive from application of a thin gold layer by sputtering, and needs to be kept in a vacuum.

2.5.3 Scintillation counter

A simple way of measuring the permeability of a polymeric film is by using a radioactive diffusant such as tritiated water. The simplicity derives from the ease of measuring the concentration of the diffusant by using a scintillation counter, since the radioactivity is proportional to the concentration of diffusant [21]. Since the concentrations of the diffusants in this case are very low, the film will not be subjected to high osmotic pressure and due to the lack of a large concentration gradient the diffusion can be approximated to be self-diffusion of the molecule alone.

Samples are analyzed for their radioactive content by liquid scintillation counting. The counter works by detecting luminescence created by the radiation from the radioactive diffusant. In order for this to occur a specific liquid solution of different organic materials (scintillation cocktail) needs to be added to each sample [21]. The scintillation cocktail contains a fluorescent molecule (scintillator) and surfactants in an aromatic solvent.

Tritium (^3H) is a radioactive isotope of hydrogen including not only the proton, but also two neutrons in the hydrogen nucleus. Tritiated water is simply a water molecule including this heavy hydrogen instead of the generally occurring hydrogen (^1H). The tritium radiation is very low in energy and is only potentially dangerous if inhaled or digested. In the form of tritiated water it may also be absorbed by the skin [22].

3 Experimental

3.1 Materials

Hydroxypropyl cellulose (Nisso HPC) of four different viscosity grades (Table 1) were supplied by Nippon Soda Co. Ltd, Japan. Ethyl cellulose of viscosity grade 10 cps was supplied by Dow Wolff Cellulosics GmbH, Germany. The molecular weight and hydroxypropyl content of the polymers are shown in Table 1. A complete record of the different polymers is presented in Appendix I.

Table 1: Record of molecular weight and hydroxypropyl content for the different polymers. Data as supplied by the manufacturers.

Polymer	Manufacturer	$M_w/10^3$	Hydroxypropyl content (%)	Molecular substitution
EC10	Dow Chemicals	29[1)]	-	-
HPC-SSL	Nisso	40[2)]	69.4	3.24
HPC-SL	Nisso	100[2)]	69.4	3.24
HPC-L	Nisso	140[2)]	69.6	3.26
HPC-M	Nisso	620[2)]	68.1	3.11

1) Previously determined by SEC-MALS/RI
2) Manufacturer's data

The polymers described in Table 1 were dissolved in ethanol (95% v/v) supplied by Kemetyl AB, Sweden. All water used in the experiments was ultra-pure deionised water. The mobile phase for the SEC consisted of NaCl (Fluka analytical, Sigma-Aldrich GmbH, Germany) and NaN_3 (Sigma-Aldrich GmbH, Germany). The liquid used as needle wash in the auto sampler for the SEC consisted of water and analytical grade MeOH (Sigma-Aldrich GmbH, Germany) at a 50/50 ratio (v/v). The radioactive labelled molecule (tritiated water) for the permeability study (chapter 3.5.1), the scintillation cocktail (Ultima Gold Cocktail) and sample vials were supplied by Perkin Elmer Inc, USA.

3.2 Molecular weight determination

The polymers were dissolved in mobile phase (10 mM NaCl, 0.02% NaN_3) and stirred for 48 h before analysis with SEC (chapter 2.5.1). Depending on the molecular weight of the polymer the solutions were made to different concentrations (Table 2). The molecules were separated using the column TSKgel GMPWxl (TOSOH Bioscience GmbH, Germany). The detectors used were a RI (Optilab® T-rex™, Wyatt technologies, USA) and a MALS (DAWN® HELEOS™ II, Wyatt technologies, USA). Each injection (100 μL) was run for 30 min, each sample was injected three times and the volume flow through the column was 0.5 ml/min. At regular intervals a Pullulan standard (Shodex Standard P-50, Showa Denko Europe GmbH, Germany) was studied for reference. The injections were performed by an autosampler (Waters 717 Autosampler, Waters corporation, USA) and the data was analyzed using the software ASTRA 5.3.4.20 (Wyatt technologies, USA) with Berry linear model, exponential mass fitting and a dn/dc value of 0.138 ml/g. The vials used in the auto injector were 700 μl polypropylene vials supplied by Scantec Lab, Sweden.

Table 2: Polymer solutions for molecular weight determination with SEC

Polymer	Concentration [mg/ml]
HPC-SSL	1
HPC-SL	1
HPC-L	0.7
HPC-M	0.5

3.3 Viscosity adjustments

In order to maintain the same process parameters when producing the polymer films (chapter 3.4) for the different molecular weight HPC the viscosity was adjusted to be within the same range. This was done in order to avoid the viscosity to be a parameter for the spraying, as the polymer solutions are subjected to high shear in the spraying nozzle. The measurements were performed using a rheometer (AresG2, TA instruments) and adjusting the polymer content until the viscosity was within 50-65 mPa, which has been shown to be adequate viscosities in prior film preparations [3].

Practically, stock solutions of the polymers were prepared by dissolving the polymers in ethanol (95% w/w) to yield solutions with 6-10% w/w polymer (70% w/w EC10 and 30% w/w HPC) content, depending on the molecular weight of the polymers. The solutions were stirred (1000 rpm, magnetic stirrer) for 24 h to ensure complete dissolution of the polymer before the viscosity was measured. A flow curve was constructed by varying the shear rate from low to high (0.1 – 1000 s^{-1}) and back whilst measuring the viscosity. The higher shear rates are most important for this application since during the spraying process the solutions are going to be subjected to high shear in the nozzle. The reversed measurements are performed to assure that the solution does not exhibit thixotropic behaviour.

The viscosity measurements were analyzed using the software TA instrument Trios (version 1.8.6.892). The geometry of a concentric cylinder (Table 3) was used due to this geometry's smaller surface from which the solvent could evaporate, which is important to maintain the same polymer concentration of the solution. Immediately before the measurements the polymer solution (6.7 cm^3) was added to the cylinder, in order to avoid solvent evaporation.

Table 3: Dimensions of geometry (concentric cylinder) for viscosity measurements

Bob diameter	18.597 mm
Bob length	27.862 mm
Cup diameter	19.99 mm
Minimum sample volume	6.56842 cm^3

3.4 Film preparation

For the free film preparation an instrument (Gandalf II, earlier described in literature by Jarke [23]) designed by AstraZeneca to mimic a fluidized bed and the application of polymer films on pellets was used. The polymer solution was sprayed through a nozzle on to a rotating drum (214 cm^2, 80 rpm) that was kept in a tempered airflow. The nozzle was, whilst spraying, moving horizontally back and forth (1.3 cm/s) to spray the drum evenly. As the solution was sprayed the ethanol was evaporated and a polymer film was created on the drum. Images of the setup can be seen in Figure 3. After the spraying process was finished the film was kept in the drum until dried with the airflow temperature set to 50°C.

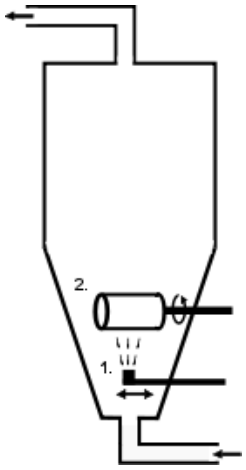

Figure 3: Schematic illustration of the spraying equipment where 1. is the nozzle, which is moving back and forth during spraying and 2. is the rotating drum. A heated airflow is applied through the equipment as by the arrows.

The polymer solutions were prepared by dissolving the polymers (30% w/w HPC, 70% w/w EC10) in ethanol at the concentrations determined by the viscosity adjustment (chapter 3.3) and stirred with 1000 rpm for minimum of 24 h to ensure complete dissolution.

The process parameters with which the films were sprayed can be seen in Table 4. The aim was to keep these as similar as possible for the different films in order to avoid diversity to evolve from the spraying process. The actual process parameters for each film are shown in Appendix II.

Table 4: Process parameters for film spraying

Air flow	40.0 m^3/h
Air flow temperature	72.0°C
Atomizer pressure	2.00 bar
Atomizer flow	1,93-1.99 bar
Spray rate	12.9-14.4 g/min

Each film had a dry weight of 6.2 g of polymer to achieve an approximate thickness of 150 μm. This thickness was chosen in order to achieve concentrations of HPC above the RI detection limit from the HPC leaching experiments (chapter 3.5.2).

3.5 Diffusion cells

The permeability of the different films was measured using an Ussing chamber (side-by-side diffusion cell) earlier described by Hjärtstam et al [24] and a radioactively labelled diffusant (tritiated water). As can be seen in Figure 4 the diffusion cell consists of two compartments joined by a tube, in this tube the film of interest is attached and all diffusion between the two containers had to pass over this film. The thickness of the film was measured at five places and the weight of the film piece was recorded before and after the diffusion experiment.

The permeability was measured by measuring the radioactivity in the receiver cell, which was directly proportional (chapter 2.5.3) to the diffused mass from the donor cell to the receiver cell over the film. Rapid stirring was applied to both cells to avoid the formation of a stagnant layer of dissolved HPC in the film region and to create an as uniform solution as possible regarding temperature and solutes.

The whole system was surrounded by a water jacket (37°C) in order to perform the measurements at a temperature corresponding to that of the human body. Both stirring rate and temperature was monitored carefully as they could have significantly affected the results [2].

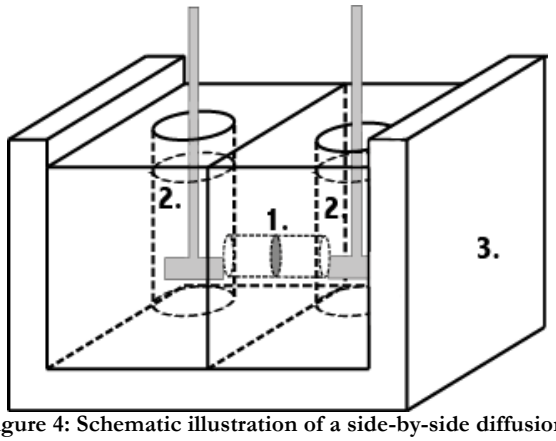

Figure 4: Schematic illustration of a side-by-side diffusion cell. 1. Free polymer film, 2. Donor- & receiver cell, 3. Water jacket

3.5.1 Permeability measurements

For the permeability measurements small film pieces (approximately 1.5 cm by 1.5 cm) were carefully examined for cracks and then mounted between the compartments of the preheated Ussing chamber and after 10 min both cells were simultaneously filled with dissolution media (15 ml, 37°C). The dissolution media was the same salt solution that was used as elution media in the SEC (10 mM NaCl and 0.02% NaN_3). After a specific period of time (1 min) the radioactive tracer (10 µl, 400 Bq) was added to the donor cell and the measurement started. At regular intervals small samples (500 µL) were removed and readily replaced by the same amount of dissolution medium in order to disturb the system as little as possible. The samples were carefully weighed to determine the exact volume that was withdrawn and then analyzed using a liquid scintillation counter (Tricarb Liquid Scintillation Analyzer B2810R, Perkin Elmer).

One minute after the tracer was added the system was considered to be uniform and a reference sample for tritium activity determination was taken from both compartments of the cell. These samples were not replaced with new dissolution medium. The initial sample from the donor cell had a very high radiation content and was therefore be diluted 100 times prior to analysis. The radioactivity in the receiver cell was proportional to the diffused mass of radioactive tracer, which means that the diffusion through the film could be calculated. The measurements were conducted for 24 h with samples every 15 min for the first 100 min, every 30 min for the first 4 h and then once an hour up to 6h. The final samples were taken the next day, a total of three samples at intervals of 30-60 min. The samples taken the day after were only to conclude if there was any change in permeability after the initial 6 h and if this was consistent with the permeability measured after 24 h of HPC leaching (chapter 3.5.2).

3.5.2 HPC leaching experiments

In order for the leaching experiments to be directly comparable with the earlier described permeability experiments (chapter 3.5.1), these experiments mimicked that procedure with the exception of samples being taken from both the donor and the receiver cell. At the end of the experiment the dissolution media in the cells was replaced by new dissolution media (15 ml, 37°C) and a finalizing permeability experiment for the fully permeable film was performed in order to be compared with the results from the original permeability experiment.

The film densities were determined by measuring the volume of a film piece and registering its weight, this was done in replicates of three for each film. The volume of the cut out film pieces was determined by measuring the length, width and thickness at five different places of the film using a micrometer. The film densities were used to determine the maximum theoretical amount of HPC in the volumes of the film that were subjected to water. This was done in order to be able to compare this with the detected amounts of leached HPC from the films.

The leaching rate was calculated by approximating the slope in each measure point. This was done according to the following equation:

$$\frac{dc_i}{dt} = \frac{c_{i+1} - c_{i-1}}{t_{i+1} - t_{i-1}}$$

where dc/dt is the leaching rate, t is the time and c is the concentration of leached polymer adjusted for theoretical available amount.

All films that were subjected to water in the diffusion cells (permeability and HPC leaching experiments) were weighed before the experiments were conducted. This weight was then compared to the weight of the film piece after exposure to water, in order to approximate the HPC leaching by weight loss of the film. The films were dried for several days in a dessicator prior to weighing to ensure the same moisture content.

3.5.2.1 SEC-RI

For measuring the concentration of HPC in the samples the same water phase size exclusion chromatography as described in chapter 3.2 was used together with a RI detector (Optilab® T-rex™, Wyatt technologies, USA). In order to define the detection limit of HPC for the RI detector a dilution series of concentrations ranging from 0.0005 mg/ml to 1 mg/ml of HPC-SSL was prepared and analyzed using the above mentioned equipment. Three injections of each sample were analyzed.

3.6 SEM imaging

The micro structural properties of the EC/HPC films were, in order to determine possible structural differences between the different molecular weight HPC, studied using a field emission SEM, Leo Ultra 55 FEG SEM (LeoElectron Microscopy Ltd, Cambridge, UK), by in-line detection mode at 3 kV. The EC/HPC films were studied both after being exposed to water and not exposed to water at all in order to study the pore sizes after the HPC had leached out and to see if there were any microstructure present due to the film spraying method.

3.6.1 Sample preparation

Six different samples of each film were investigated using SEM. Surfaces of films exposed to water during permeability experiments, films that were not exposed to any water and cross sections of films exposed to water. The cross sections were prepared by immersing the films from permeability experiment in liquid nitrogen and whilst still frozen breaking these by bending. Half of the broken films were then exposed to water a second time by adding the film pieces to a 12 well culturing plates together with 5 ml deionised water and placing this in a preheated (22.5 h, 37°C, 350 rpm) thermoshaker, Grant-bio Thermoshaker PHMP-4 (Grant Instruments Ltd, Cambridge, UK). This was done in order to expose the cross-section to water and then visually determine if any HPC had been enclosed in EC and unable to leach out in the diffusion cells. After leaching the film samples were dried in a dessicator for 48 h to eliminate residual water that would interfere with the SEM measurement.

The fractured surfaces were cut off to form thin (1-2 mm) pieces, which were adhered “standing up” on conductive carbon tape with the fractured surface pointing upwards. The area

exposed to water by the permeability experiments was noted in order to differentiate between the cross section surfaces of the film areas exposed to water and film areas not exposed to water.

The film surfaces were finally coated with gold by ion sputtering in order to create a conductive surface for SEM imaging. After gold sputtering the samples were kept in a dessicator until studied using SEM.

4 Result

4.1 Molecular weight

The molecular weights, determined by SEC (chapter 3.2), of the different HPC are shown in Table 5 together with the data supplied by the manufacturer. Although not noted by the manufacturer, it seems that the molecular weight is given as the z-average molecular weight, M_z. The polydispersity index (PI), defined as M_w/M_n, is also noted here.

Table 5: Molecular weights of the different HPC. Both according to manufacturers' data and determined by SEC. The molecular weight and polydispersity index are results of one sample analyzed in three replicates.

Polymer	$M^{1)}/10^4$	$M_z^{2)}/10^4$	$M_w^{2)}/10^4$	$PI^{2)}$
HPC-SSL	4	4.6	3.1	1.5
HPC-SL	10	8.5	5.6	1.6
HPC-L	14	13.1	8.3	1.8
HPC-M	62	62.3	37.5	2.4

1) Manufacturer's data
2) Determined using SEC

For all but one type of HPC, a bimodal molecular weight distribution was present when the molecular weights were investigated as can be seen in Figure 5. The molecular weights represented by each of these peaks are presented in Table 6.

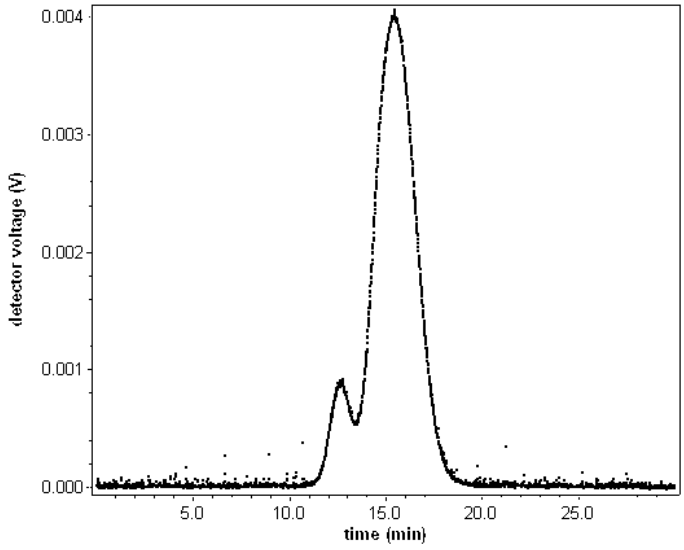

Figure 5: Example of the bimodal molecular weight distribution of HPC-L, HPC-SL and HPC-SSL. The graph is from the molecular weight determination of HPC-SSL. The graph shows the MALS detector output with detector voltage against elution time.

Table 6: The molecular weight of the two different peaks of the bimodal weight distribution that are displayed in Figure 5.

Polymer	$M_w/10^6$ (peak 1)	$M_w/10^6$ (peak 2)
HPC-SSL	1.5	0.031
HPC-SL	2.1	0.055
HPC-L	1.9	0.082

The result of the analyzed dilution series of HPC-SSL (Table 7) gave the detection limit for the RI to be around 0.005 mg/ml.

Table 7: Displaying the yield of the detected amounts of injected mass for various dilutions of HPC-SSL. Standard deviation is given in parenthesis. For the lower concentrations no detection of HPC-SSL was possible. Each sample was analyzed in replicates of three.

Polymer	Concentration [mg/ml]	Yield [%]
HPC-SSL	1	100 (5.3)
	0.5	104 (0.5)
	0.1	104 (0.8)
	0.05	105 (2.8)
	0.01	111 (11.0)
	0.005	117 (8.5)
	0.001	-
	0.0005	-
	0.0001	-

4.2 Viscosity measurements

The viscosity of the polymer solutions after adjusting the polymer concentration is shown in Figure 6. All viscosities are present within the limits of 50-65 mPa.

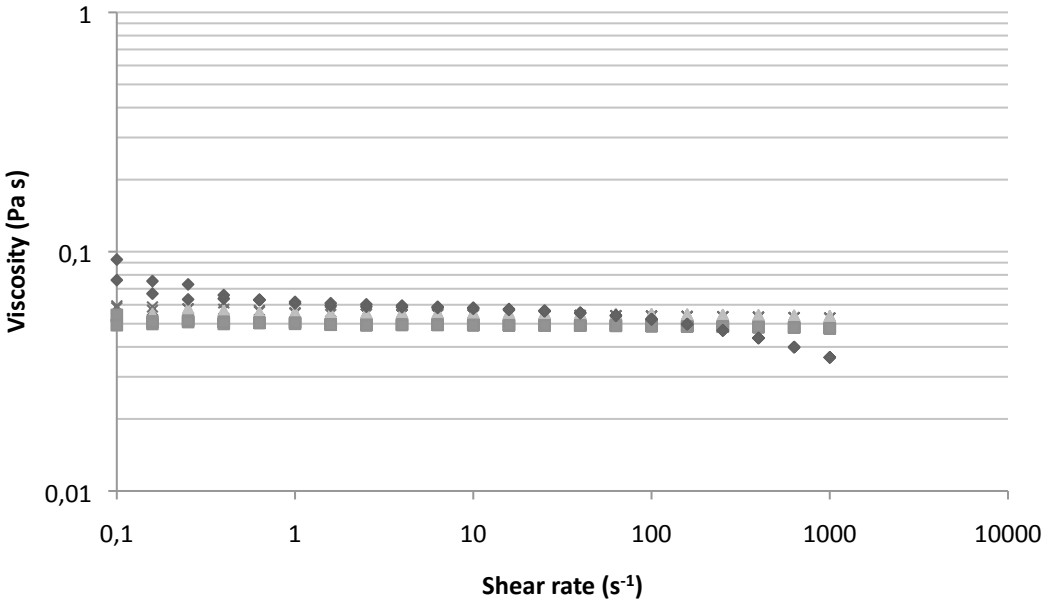

Figure 6: Viscosity of polymer solutions for film spray with adjusted polymer concentration. All viscosities were within 50-60 mPa for the major part of the shear rate sweeps. The results are from one replicate. ◆ HPC-M, ■ HPC-L, ▲ HPC-SL, ✕ HPC-SSL

4.3 Sprayed films

Images of the sprayed films are given in Appendix III. From these images it is possible to see the macrostructure of the sprayed films. The films made of EC10/HPC-M and EC10/HPC-L show a smooth film structure, but the films made of EC10/HPC-SL and EC10/HPC-SSL display small bubbles and dried particles at the surface.

The temperatures during the sprayings are shown in Figure 7 as the temperature of the gas outflow from the spraying equipment. This temperature relates to the temperature at the sprayed surface. The temperature is important for the phase separation, as the temperature of the newly sprayed surface controls the solvent evaporation.

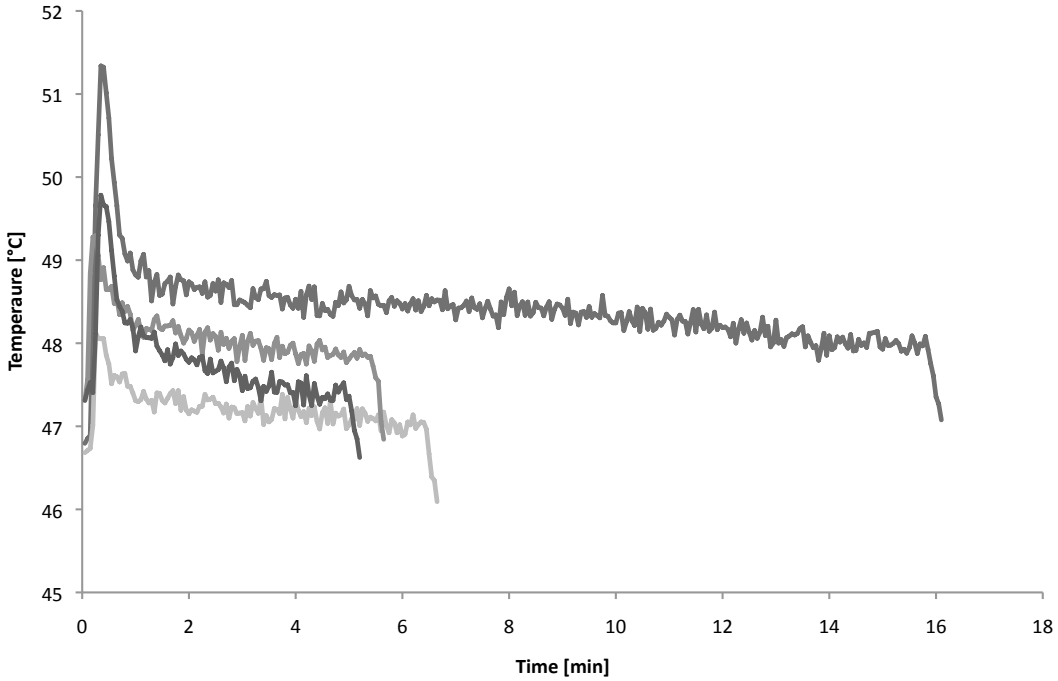

Figure 7: The temperatures of the airflow out of the spraying equipment for the films used in this study. These temperatures are related to the temperatures at the film during spraying and are therefore important for the phase separation. From top to bottom HPC-M, HPC-SL, HPC-SSL, HPC-L.

4.4 Permeability

A comparison of the permeability for the different molecular weights of HPC is shown in Figure 8 together with the same comparison for lag-time. The permeability and lag-time is illustrated as a function of increasing molecular weight.

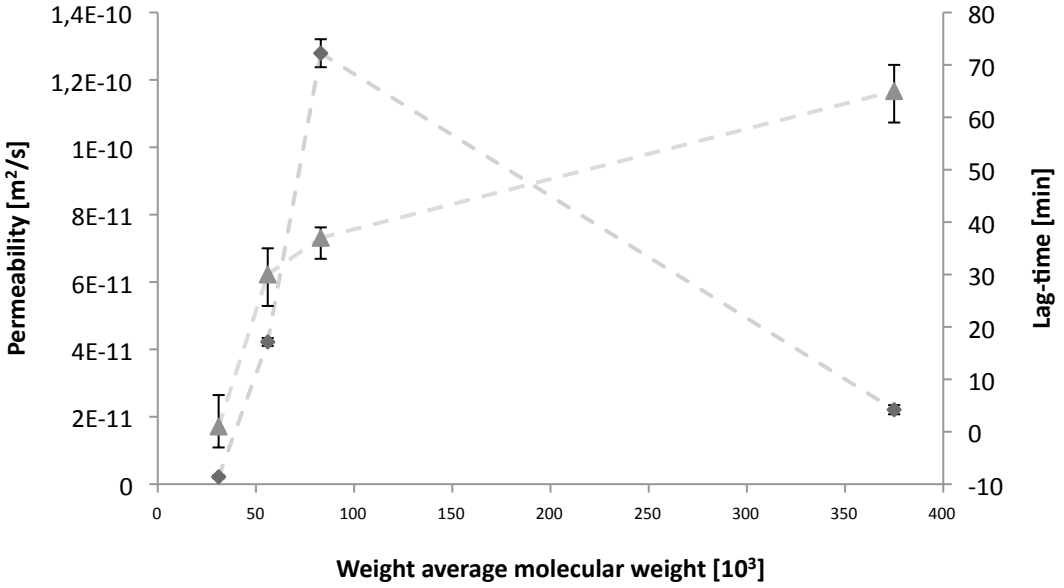

Figure 8: The permeability (◆) and lag-time (▲) of the EC/HPC films shown as a function of increasing molecular weight HPC.

The diffused mass (% of available amount) as a function of time for the medium molecular weight HPC (HPC-L) is shown in Figure 9 as a reference of what the permeability measurements looked like. The lag-times, calculated from the linear regression of the mass

transfer through the films (shown in Figure 9), are displayed in Table 8 together with the permeability of the films and the permeability measured after 24 h of leaching experiments.

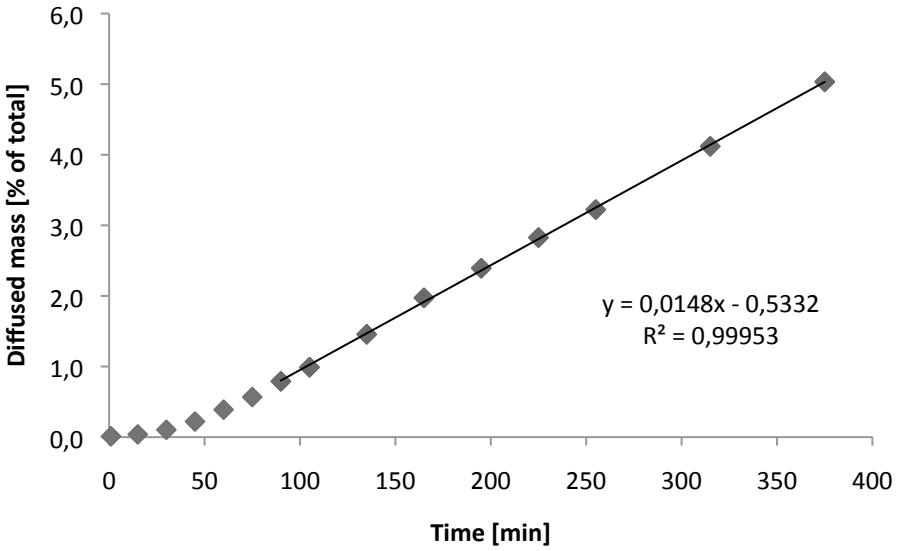

Figure 9: Increasing concentration of radiolabeled molecule in the acceptor chamber of the diffusion cell, shown as a function of time. The equation for the linear regression, from which the lag-time is calculated, is also displayed.

Table 8: The lag-times (calculated from the linear regression illustrated in Figure 9) and permeabilities for the films with different molecular weights HPC. The permeabilities are also illustrated in Figure 8 as a function of molecular weight. The experiment was performed in replicates of three and standard deviation is given in parenthesis.

Film	M_w /10^4	Lag-time [min]	Permeability [10^{-10} m^2/s]	Permeability leached film [10^{-10} m^2/s]
EC10/HPC-SSL	3.1	1 (4.9)	0.022 (0.0043)	0.018 (0.0032)
EC10/HPC-SL	5.6	30[1)] (5.0)	0.42[1)] (0.0083)	0.58 (0.023)
EC10/HPC-L	8.3	37 (2.9)	1.3 (0.042)	1.1 (0.080)
EC10/HPC-M	37.5	65 (5.7)	0.22 (0.014)	0.51 (0.011)

1) Measured for two replicates. The values are given as averages and the deviation is given in parenthesis.

4.5 HPC leaching

Figure 10 shows the, by SEC detected (chapter 3.5.2), concentrations of leached HPC over time. The amount of HPC is illustrated as percentage of maximum possible amounts of HPC calculated by determination of film density and the film volume exposed to water in the diffusion cells. The presented results are based on two replicates. No detection of HPC-SSL was possible using this method, due to concentrations being below the detection limit of the RI detector. What should also be noted is that for two of the films (containing HPC-SL and HPC-L) the detection of HPC is well above 100% of the theoretical amount. The calculated film densities are presented in Table 9.

Table 9: The densities of the different EC/HPC films. The density was calculated for three replicates, standard deviation is given in parenthesis. The thicknesses of the different films are also presented here.

Film	Thickness [µm]	Density [mg/mm^3]
EC10/HPC-SSL	177 (6.7)	1.08 (0.0052)
EC10/HPC-SL	153 (2.6)	1.08 (0.026)
EC10/HPC-L	150 (2.1)	1.10 (0.0068)
EC10/HPC-M	148 (2.6)	1.11 (0.0032)

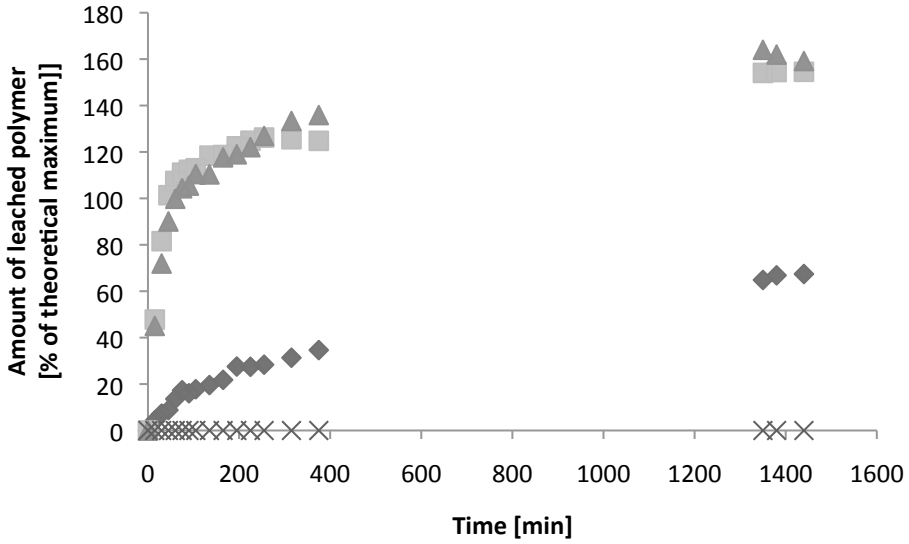

] HPC is shown as a percentage of the theoretical maximum amount present in the film pieces. ◆ HPC-M, ■ HPC-L, ▲ HPC-SL, ✕ HPC-SSL

The leakage of HPC was measured for both sides of the films (Figure 10 shows the total leakage for the film) and this is shown in Figure 11. There is a small difference between the two sides for HPC-L and HPC-M but a large difference for HPC-SL.

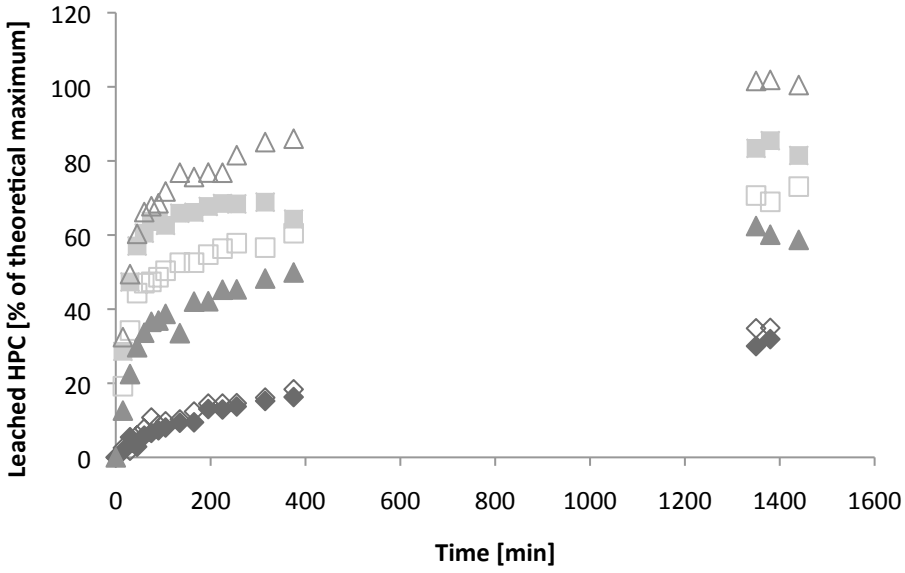

Figure 11: The HPC leakage from the film as a function of time shown as leakage detected in the individual cells (donor cell – filled symbols; receiver cell – empty symbols), in other words the leakage from each side of the film. Results are from one replicate. ◆ HPC-M, ■ HPC-L, ▲ HPC-SL.

The rate with which the leaching of the HPC from the EC/HPC films occurs is presented in Figure 12. Since no HPC-SSL could be detected, as seen in Figure 10, these results have been left out from this graph.

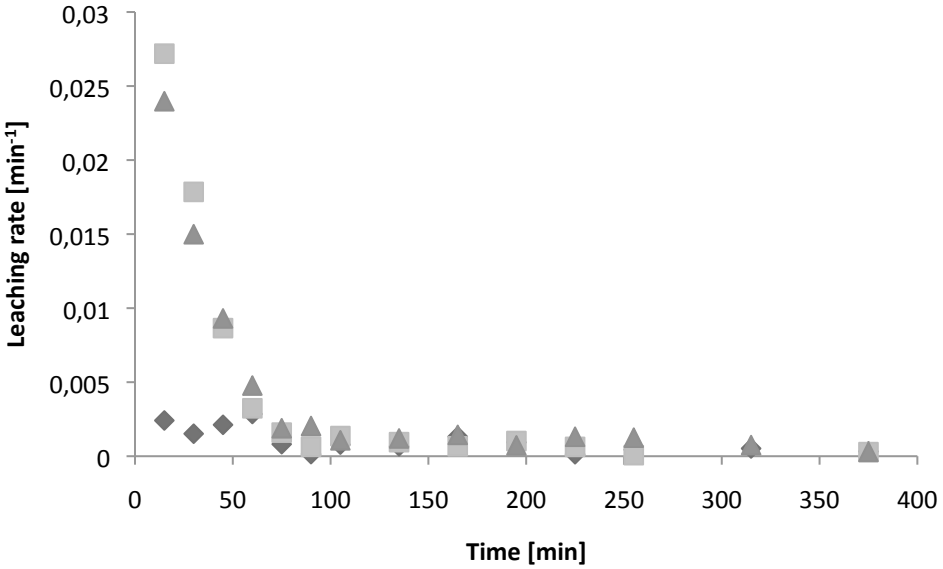

Figure 12: The rate of leaching of HPC from the different EC/HPC films. Since no leaching of HPC-SSL could be detected using SEC (Figure 10) this result has been left out from this graph. ◆ HPC-M, ■ HPC-L, ▲ HPC-SL

The total amount of leached HPC from the EC/HPC films is displayed in Figure 13 and Table 10. The amount of leached HPC is also represented by the weight loss of the films proportional to the theoretical maximum amount of HPC in the EC/HPC film pieces (Figure 14). Note that these values are well above 100% of theoretical weight loss. Note also that the values for HPC leakage acquired from the weight loss of the films are somewhat higher than those acquired from HPC detection using SEC-RI.

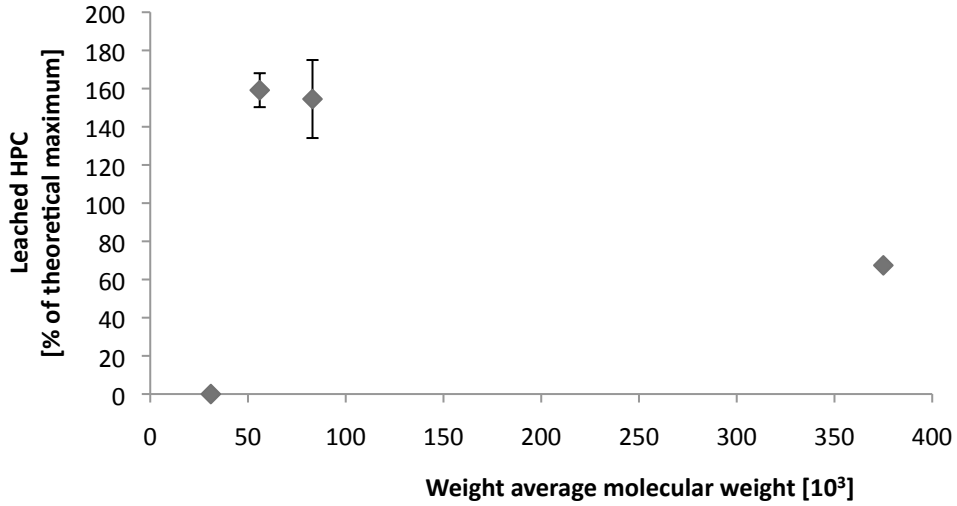

Figure 13: Total amount of leached HPC for the different EC/HPC films after 24 h of exposure to water in the diffusion cells. The results are from one replicate and the average of two injections. The error bars display the maximum and minimum detection. The total amount of leached HPC is also presented in Table 10.

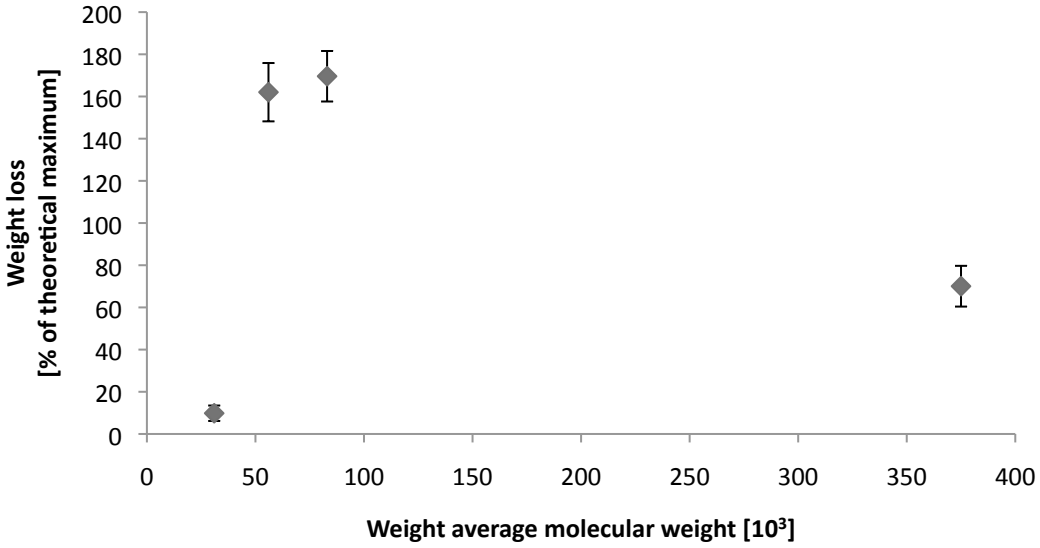

Figure 14: The weight loss for the different films after 26 h of leaching presented as a percentage of maximum theoretical amount of HPC in each film, assuming all weight loss is due to loss of HPC. Weight differences calculated for replicates of 6 and the error bars show the standard deviation.

Table 10: The total amount of leached HPC after 24 h, presented as a percentage of the theoretical maximum amount of HPC present in the different films. The results are presented graphically in Figure 13. Measurements were performed in replicates of one and are the averages of two injections. The deviation is given in parenthesis.

Film	Total amount of leached HPC [% of theoretical]
EC10/HPC-SSL	-
EC10/HPC-SL	159 (8.9)
EC10/HPC-L	154.5 (20.4)
EC10/HPC-M	67.4 (0.88)

1) No detection, sample concentrations below detection limit.

In Figure 15 the amount of leached HPC from the films are presented as a function of permeability. Linear regression of the measure points for the different films are also shown together with the equation and R^2 value. A linear behaviour can be seen, except for the varying permeability in the later samples of HPC-L.

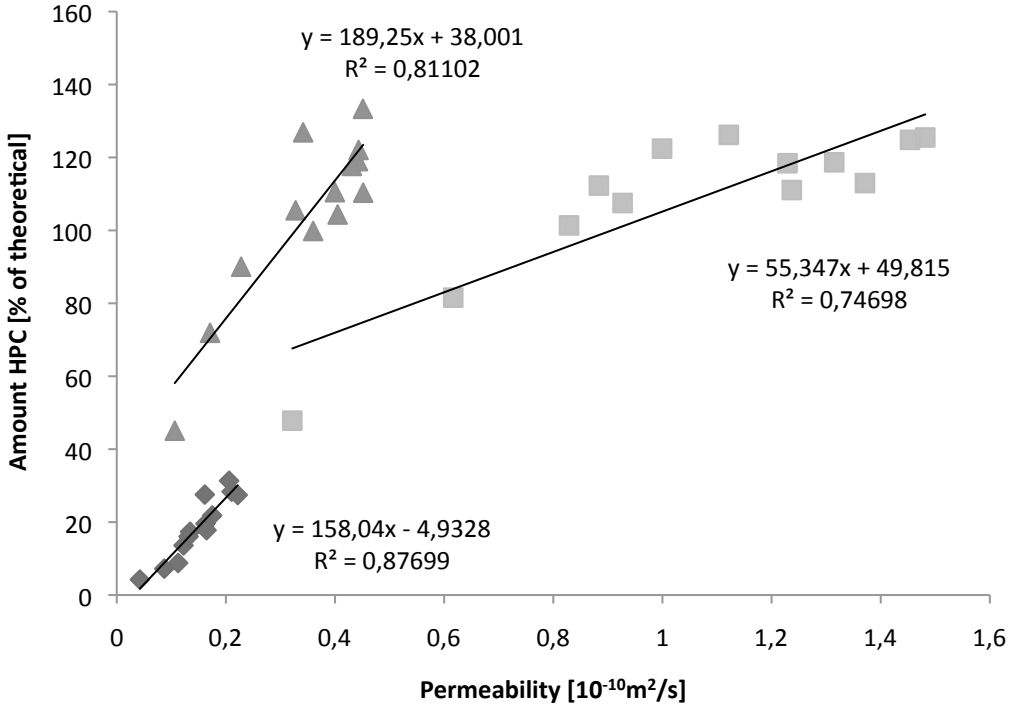

Figure 15: Graph displaying the leached amount of HPC as a function of permeability for the samples taken within 6 h from the beginning of the experiment. The linear regression for each sample series is also denoted in the graph together with the R^2 value. ◆ HPC-M, ■ HPC-L, ▲ HPC-SL

Table 11 shows the approximated amount of HPC that has leached from the films at the, from permeability experiments determined, lag time. The result is presented as a percentage of the total amount of leached polymer detected after 24 h of exposure to water.

Table 11: The amount of leached HPC at the lag-time for the different film. The result is presented as a percentage of the total amount of detected HPC after 24 h (Table 10)

Film	HPC leached at lag-time [% of total]
EC10/HPC-SSL	-
EC10/HPC-SL	45
EC10/HPC-L	59
EC10/HPC-M	22

4.6 SEM imaging

4.6.1 Surface

SEM images of the outer and inner surfaces of the films, from production, are shown in the following segment. Figure 16 shows the inner surfaces of the films, after being exposed to water, at different magnifications and Figure 17 shows the outer surfaces of the same films. From these images it is clear that the outer surfaces contain much more pores than the inner surfaces. Among the films similar structural properties (pore size and pore distribution) can be observed for the films containing HPC-SL and HPC-L (Figure 16 a-f and Figure 17 a-f). Films

containing HPC-M show the smallest pore size, followed by HPC-SSL and the largest pore size is present in films containing HPC-L followed by HPC-SL.

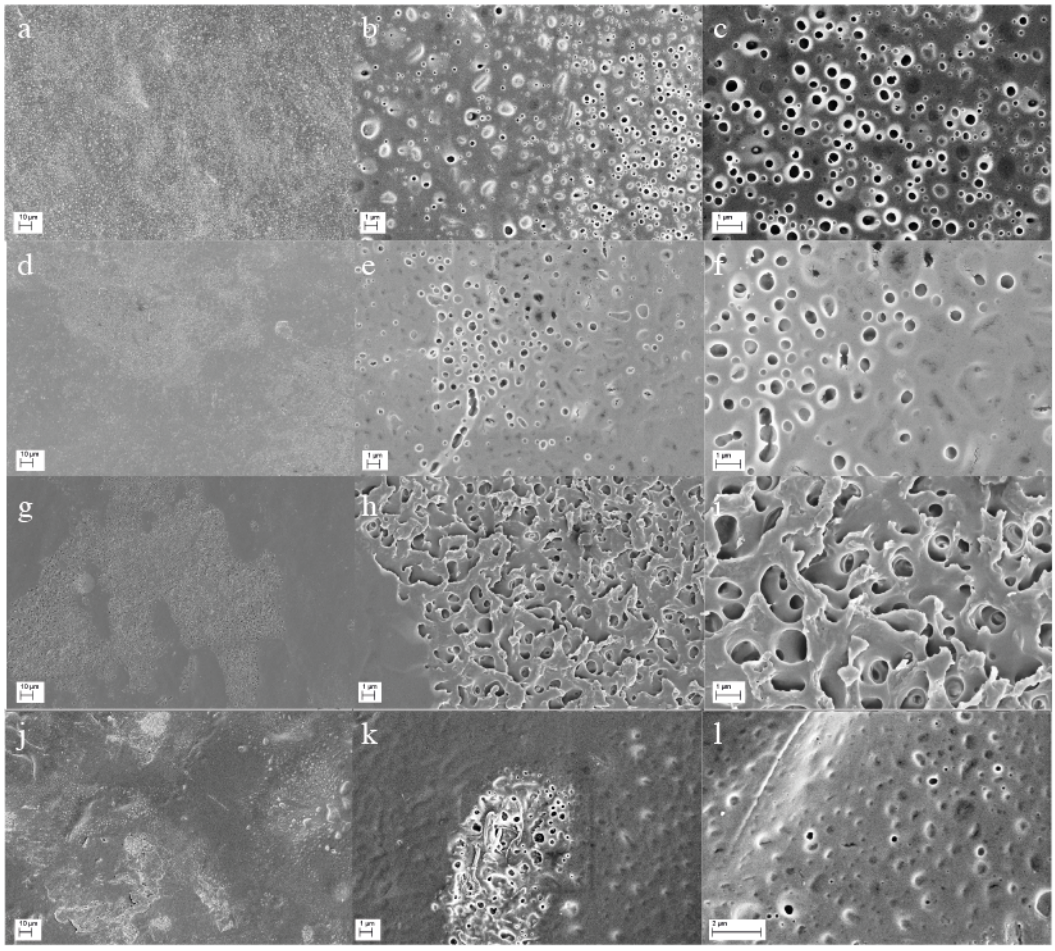

Figure 16: SEM images of the drum side of all films. From the top HPC-SSL, HPC-SL, HPC-L and HPC-M. All films are shown with (from left to right) magnifications of 1000x, 10 000x and 20 000x. The scale bars show (from left to right) 10 µm, 1 µm and 1 µm, except for the scale bar in figure l, which show 2 µm.

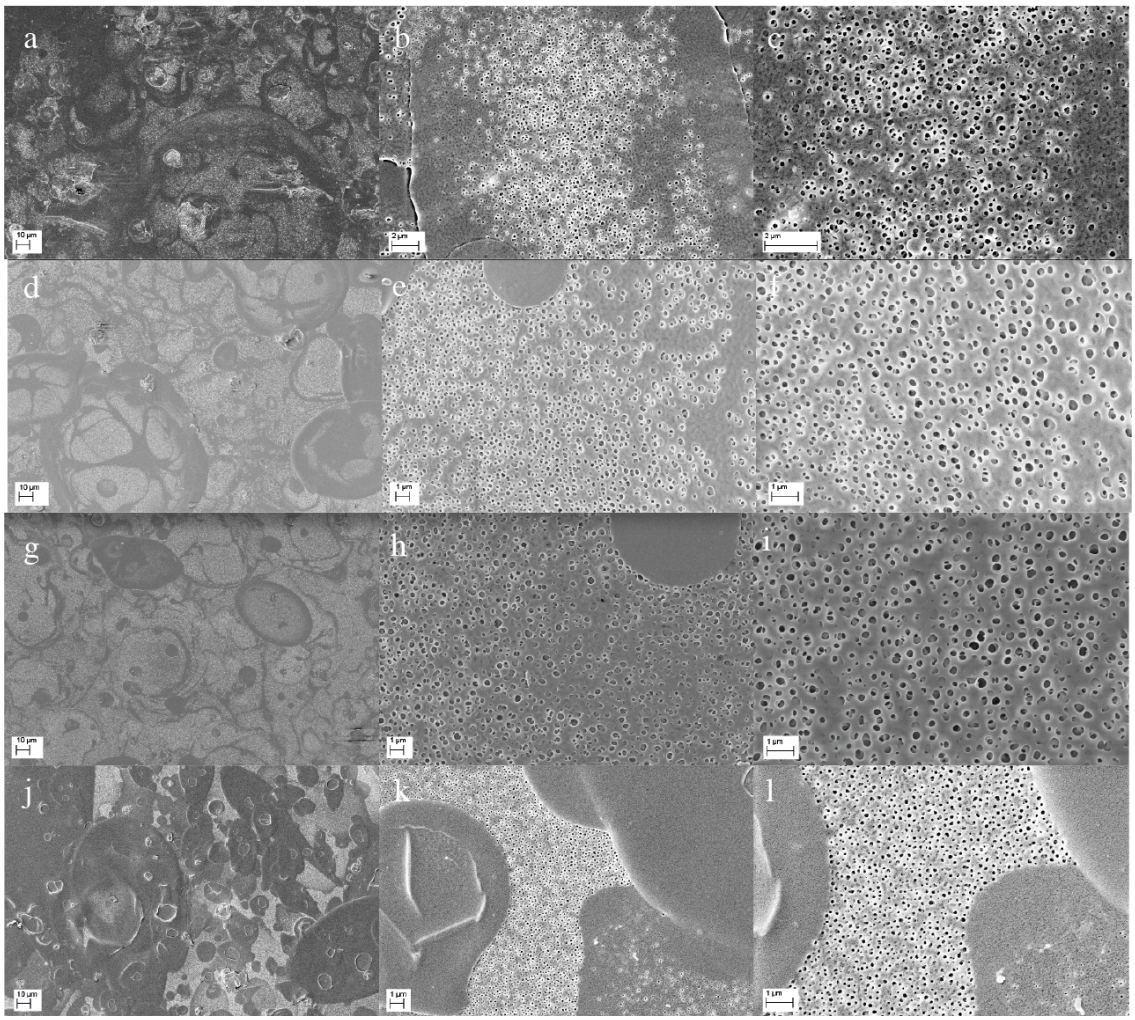

Figure 17: SEM images of the air surface (in film production) of all films. From the top HPC-SSL, HPC-SL, HPC-L and HPC-M. All films are shown with (from left to right) magnifications of 1000X, 10 000x and 20 000x. The scale bars show (from left to right) 10 µm, 1 µm and 1 µm, except for the scale bar in figure a, b and c, which show 20 µm, 2µm and 2 µm respectively.

Figure 18 shows the outer and inner surfaces of the films directly from production that is not exposed to water. From these images it is possible to see that the inner surfaces, which were facing the drum during the film production, of the films are generally smother than the outer surfaces of the films. Also HPC-SSL and HPC-M shows a smother structure than HPC-SL and HPC-L.

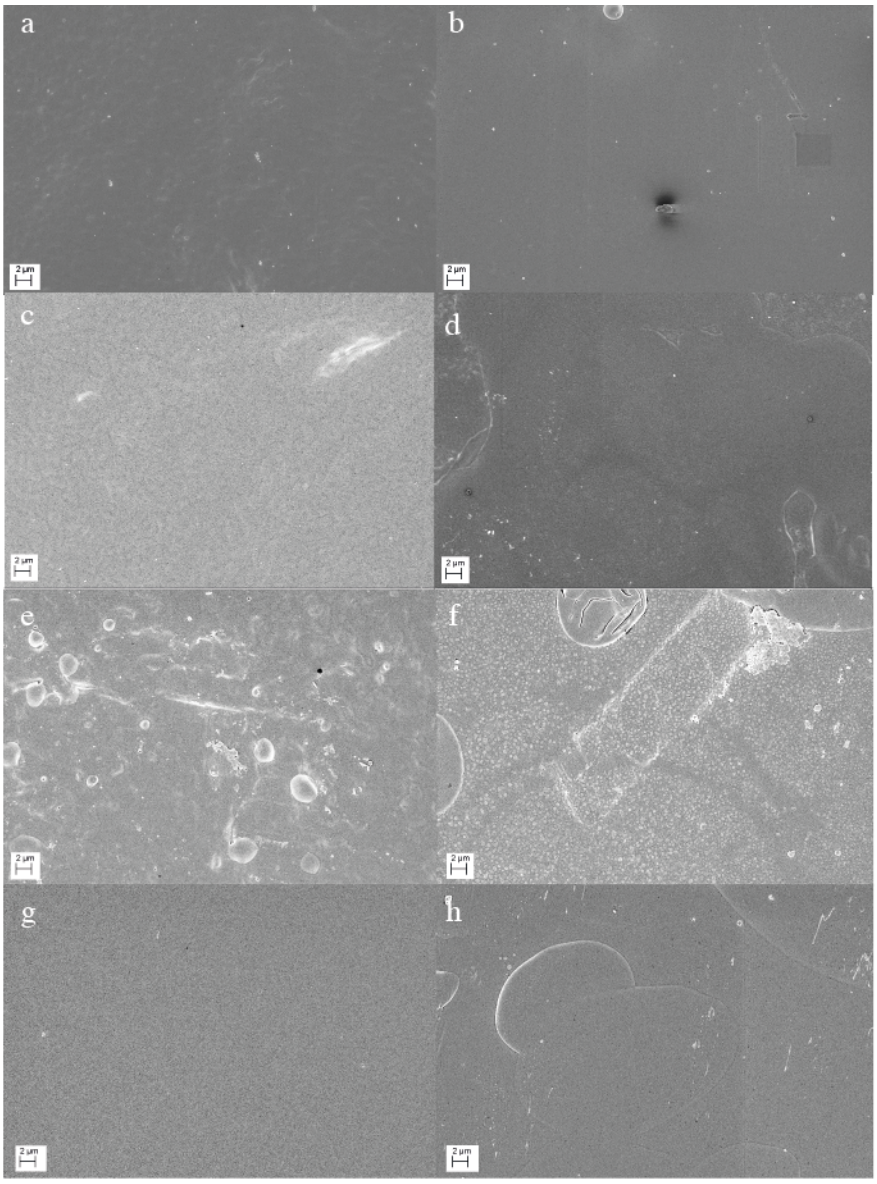

Figure 18: SEM images of all films directly from production, without exposure to water. From the top: HPC-SSL, HPC-SL, HPC-L, and HPC-M. The images to the left show the surface from the drum side in the film production and to the right is the air/spray side surface in the film production. The scale bars show 2 μm.

4.6.2 Cross section

Figure 19 and Figure 20 show cross-sectional images of the films with the lowest permeability (HPC-SSL and HPC-M). The left images show the films that were not exposed to water. The middle images show the films that were exposed to water during the diffusion experiments, which means that water was only present at the two surfaces. The right images show the films where the cross-sections were exposed to water and all HPC present at the surface could leach out. In Figure 19 a difference can be observed between the three images. The image of the film that was exposed to water in the diffusion cells (middle) shows a more porous structure than the film that was not exposed to water at all. This film, however, show a less porous structure than the image of the film where the cross section was exposed to water a second time (right). In Figure 20 to Figure 22 the same structural differences between the middle and right images cannot be observed for HPC-M, HPC-SL and HPC-L respectively. All films have a somewhat porous structure already before exposed to water (left).

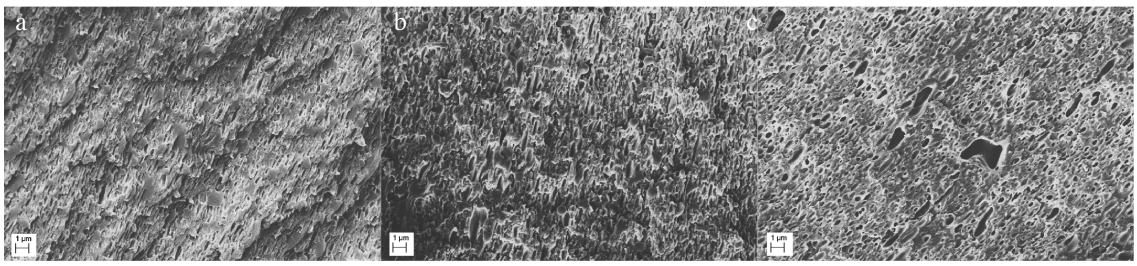

Figure 19: Images of the cross sections of a HPC-SSL film. a) is a cross-sectional image of a film that was not in contact with water, b) is a image of a film that was exposed to water in the diffusion cell and c) is a image of a film where the cross section was exposed to water. All images are of 10 000 times magnification and the scale bar show 1µm.

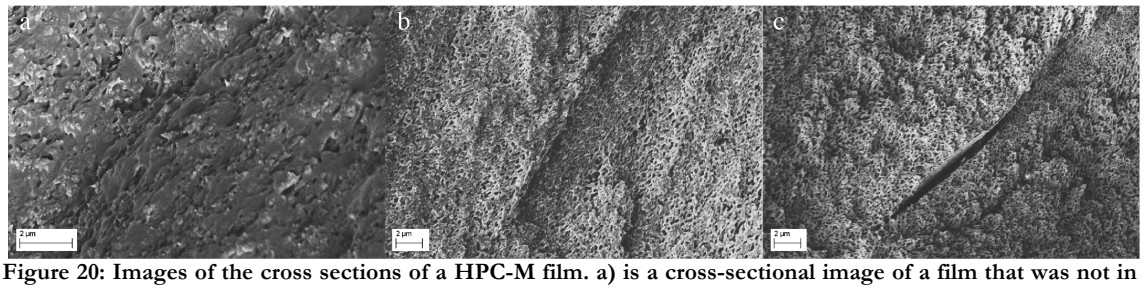

Figure 20: Images of the cross sections of a HPC-M film. a) is a cross-sectional image of a film that was not in contact with water, b) is a image of a film that was exposed to water in the diffusion cell and c) is a image of a film where the cross section was exposed to water. All images are of 10 000 times magnification and the scale bar show 2 µm, 1 µm and 1 µm respectively.

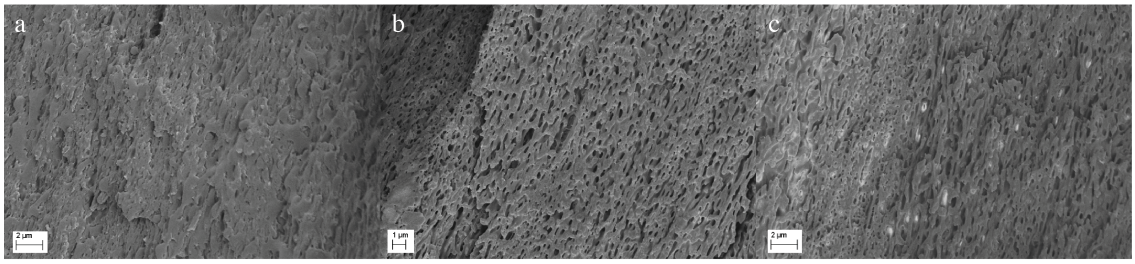

Figure 21: Images of the cross sections of a HPC-SL film. a) is a cross-sectional image of a film that was not in contact with water, b) is a image of a film that was exposed to water in the diffusion cell and c) is a image of a film where the cross section was exposed to water. All images are of 10 000 times magnification and the scale bar show 2 µm, 1 µm and 2 µm respectively.

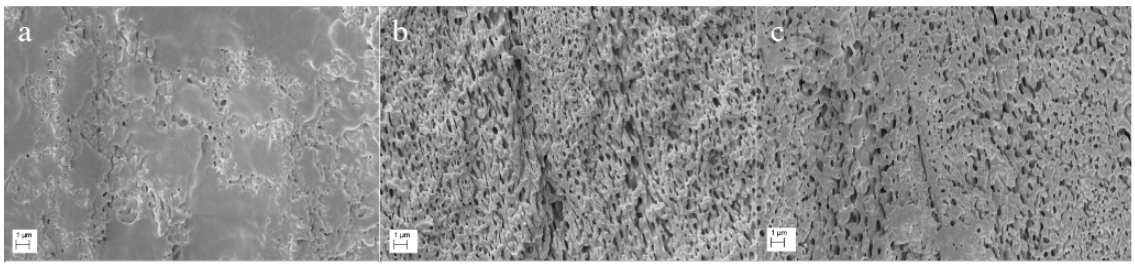

Figure 22: Images of the cross sections of a HPC-L film. a) is a cross-sectional image of a film that was not in contact with water, b) is a image of a film that was exposed to water in the diffusion cell and c) is a image of a film where the cross section was exposed to water. All images are of 10 000 times magnification and the scale bar show 1 µm.

In Figure 23 selected images showing the different part of the cross-section of the film is shown. The left image shows the inner film surface from production; here a very dense structure can be observed compared to the rest of the film. The middle image shows the bulk structure of the film with a uniformly sized porous network. The right image shows the outer surface of the film during production; here a reduced pore size could be observed. It can also be seen that the pores closest to the two surfaces exhibit an elongated shape whilst the pores in the bulk have a more spherical shape.

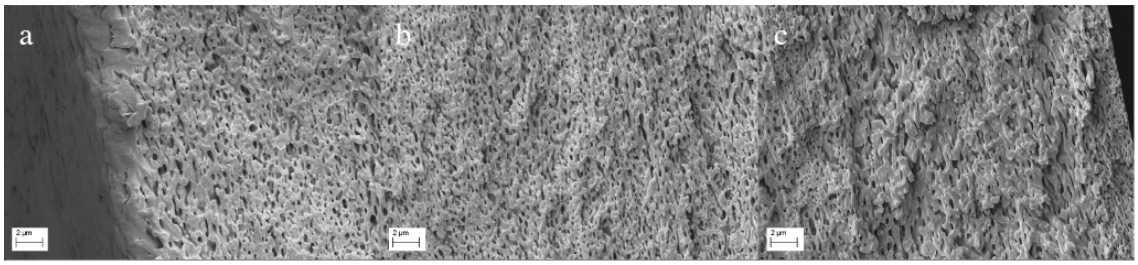

Figure 23: Images of the cross-section of a EC10/HPC-L film that was exposed to water in diffusion cells, hence HPC has leached out and formed a porous network. The images show examples of the entire cross-section with the inner surface from production (a), the bulk (b) and the outer surface from production (c). The scale bars show 2 μm.

5 Discussion

The use of free films have been shown by Wei et al to give a good estimation of the diffusion through film coated dosage forms, such as pellets, even though the processes of production is very different [25]. This means that the results from this study, which is performed on free films, are also applicable for e.g. coated pharmaceutical pellets. In order to be able to draw conclusions regarding drug dissolution from pharmaceutical pellets, however, repeated testing with a model substance is required as this may contribute in various ways.

5.1 Molecular weight influence on permeability and HPC leaching

It is obvious from Figure 8 that the films with different molecular weight HPC show different permeability behaviour, with a maximum in permeability for medium molecular weight HPC. This shows that not only the molecular weight of EC is important for the phase separation and final film structure [3], even though HPC is only present as 30% (w/w) in the films the molecular weight of HPC has an impact on the properties.

As previously mentioned, Andersson et al have shown that the molecular weight of EC affects the mass transport through EC/HPC films [3]. However, the molecular weight of EC also has an impact on the mechanical properties of the EC/HPC films, with decreasing molecular weight of EC showing decreasing mechanical properties [3]. This decrease in mechanical properties makes this approach to optimize the mass transport properties of the film unsuitable when a certain degree of mechanical properties is needed. This study shows that the molecular weight of HPC also has a strong influence on the mass transport over the EC/HPC films, and since HPC is present in a lower amount than EC this might not influence the mechanical properties to the same extent. It could therefore be beneficial for the polymer coating to change the molecular weight HPC instead of EC to yield the required mass transport properties.

The permeability dependence on molecular weight of HPC is very different from that determined for different molecular weight EC. Andersson et al noticed a decrease in permeability with increasing molecular weight EC [3], as could be seen for the highest molecular weight HPC. However, no maximum in permeability was discovered for a certain molecular weight EC. The viscosity grades of EC investigated in that study were all well below or in the lower range of the molecular weight of the HPC investigated in this study (M_w of EC100, highest M_w EC studied, was $68 \cdot 10^3$). This means that the permeability does not follow the same trends regarding molecular weight for the two different polymers, EC and HPC, but there is a significant dependence of molecular weight within each of the two polymers.

5.1.1 Low molecular weight HPC

The lowest molecular weight HPC investigated in this study ($31 \cdot 10^3$) shows the lowest permeability of them all. This can be described by multiple factors, e.g. the diffusion rate. Smaller molecules have a higher rate of diffusion than larger and the phase separation can proceed further for the smaller molecules during a certain limited period of time. It is possible that due to this, large volumes of the water soluble HPC has been enclosed in the insoluble EC and thereby never gets exposed to water. As can be seen in Figure 23 the EC has a tendency to gather at the surface of the film, which also adds to the possible enclosing of HPC within the films. Also in Figure 16 and Figure 17 this is illustrated, as the surface structures are much less porous than the internal structures (Figure 19 to Figure 22), hence less HPC is gathered at the surface.

The permeability of EC (EC 10 cps) on its own, $0.55 \cdot 10^{-12}$ m^2/s, [24], is in the same range as the permeability found for HPC-SSL. This implies that the HPC in this case have very little impact on the water permeability and nearly no porous structure is formed due to HPC leaching. This raises the question whether or not HPC-SSL has the same percolation limit as the middle range molecular weight HPC investigated by Marucci et al [2], since the continuous pores throughout the film, which benefit the permeability of the film, are not present.

When studying the cross sectional SEM images of the film containing HPC-SSL (Figure 19 a, b) the explanation of enclosed volumes of HPC is supported. Only a small difference in structure can be seen between the film that were exposed to water in the diffusion cell (b) and the film that was not exposed to water at all (a). When comparing these with the cross section of the film, which was exposed to water a second time (Figure 19 c) it is possible to see that this cross section shows a more porous structure. These differences support the theory of enclosed volumes of HPC described earlier, since most of the HPC could only leach out when the cross section was opened up (Figure 19 c). The low amount of leached HPC-SSL detected by SEC (Figure 13) and the low weight loss of the films after the diffusion experiments (Figure 14) also support this theory.

5.1.2 Intermediate molecular weight HPC

The films with intermediate molecular weights of HPC (HPC-SL and HPC-L with M_w of $56 \cdot 10^3$ and $83 \cdot 10^3$ respectively) show much higher permeabilities when compared with HPC-SSL. This correlates with the higher amounts of leached HPC detected compared to films containing HPC-SSL (Figure 13). HPC-L has the overall highest permeability in the study (Figure 8), approximately three times the permeability of HPC-SL. The HPC leaching from HPC-L and HPC-SL are very similar, which does not correlate with the larger difference in permeability just mentioned. The similarity in amount of leached HPC is however also supported by the measurements of weight loss from the films (Figure 14). When only examining the amount of leached HPC it could be assumed that these two films should have similar permeabilities due to the same amount of pores being formed. The difference in permeability between these two films can, however, be due to different structural properties that are not shown by the HPC leakage. It is possible that the EC10/HPC-SL films have formed large interconnected volumes, which does not fully penetrate the film and form pores connecting the two sides. This theory is supported by the fact that for the EC10/HPC-SL film, the differences in concentration of leached polymer between the two surfaces of the film was much larger than for the other films (Figure 11). This measurement is, however, only performed in replicates of one and in order to draw any conclusions from this further analysis needs to be performed. The difference in leakage from the two sides could be very important for actual pellet release, since then only one of the surfaces will be exposed to water and diffusion can only occur in one direction. If further analysis shows a general difference between the two sides of the films this could mean that the diffusion from the film might be much slower than expected. This could then of course have great impact on the release rate of the active substance from film-coated pellets.

5.1.3 High molecular weight HPC

The highest molecular weight HPC investigated in this study shows the second lowest permeability of all, which breaks the previous discussed pattern of permeability increasing with increasing molecular weight of HPC. The permeability measured for this high molecular weight HPC is however still higher than that of EC alone [24], which means that some pores are formed through the film. The permeability of the film is also higher than that of the EC/HPC films with

the lowest molecular weight HPC (HPC-SSL). This is supported by the amount of leached HPC, which is significantly higher than that of the lowest molecular weight HPC. These different behaviours indicates a difference in the phase separation mechanism between the two molecular weight extremes, which will be discussed later in chapter 5.6.

5.2 Total HPC leaching

Both films with HPC-SL and HPC-L display more than 100% HPC leaching when compared to the theoretical available amounts. These unreasonable results are most likely due to HPC leaching from beyond the surface open to water in the diffusion cells. With just a small increase of the radius of this surface the results are far more realistic. This diffusion beyond the established surface might also influence the result between the different films. HPC-SL and HPC-L show such similar results that the difference in water penetration most probably is very small. For HPC-M, however, the lower amount of leached polymer means that the water most likely has not penetrated as far beyond the established surface as for HPC-SL and HPC-L containing films. This influences the result by possibly increasing the difference between total leaching for HPC-M compared to HPC-SL and HPC-L by having less available HPC for films containing HPC-M. From this it can be concluded that diffusion cells are not the optimal way to measure HPC leaching behaviour since it is impossible to have a set value of HPC available in the film volume.

The percentage weight loss of the films, shown in Figure 14, is higher than the detected amounts of leached HPC in Figure 13. This difference most likely results from two things; one, it is not only HPC that leaves the polymer when exposed to water (as previously reported by Sakellariou et al [26]) and two, the concentration of HPC could be below the detection limit of the RI (chapter 2.5.1) and therefore a lower concentration is reported. Losses of EC from the films are most probably the reason for the larger weight loss than was detected as HPC leaching by SEC analysis. This is because the detection limit of the RI detector was quite low (Table 7) and the potential amounts of undetected HPC are below this limit.

5.3 Rate of HPC leaching

The leaching rate (Figure 12) is high for films containing HPC-SL and HPC-L compared to films containing HPC-M. This is consistent with the longer lag-time for films with HPC-M and the similar lag-times for films with HPC-SL and HPC-L (Figure 8, Table 8). This might be due to several things. One is difference in pore structure, with HPC-M having smaller pores and pores of different structure. Due to this the diffusion of large molecules, such as polymers, can be obstructed. As mentioned in chapter 2.3 there are different factors that affect the permeability of a porous film, such as the diffusion coefficients of the substances, the film factor describing the properties depending on the film and the hindrance factor describing the properties that are dependent on both the diffusant and the film. All these parameters of course have an impact on the leaching of HPC as well, and there is a correlation between permeability and amount of leached HPC. This as the HPC leaching is dependent on the diffusion of water into the film for the HPC to be dissolved and also the diffusion of the HPC out of the film.

Another explanation is the differences in molecular weight of the polymers. HPC-M is much heavier than HPC-L and HPC-SL and therefore exhibits a much lower rate of diffusion. The increased molecular weight also affects the dissolution properties, a longer polymer chain is less prone to be dissolved than a shorter one.

5.4 Time dependency of HPC leaching and permeability

A fairly linear behaviour of amount of leached HPC against permeability can be observed in Figure 15. What is shown in this graph is basically the dependency of porosity against

permeability. If all leached HPC forms pores connecting the two sides of the film and if the size and shape of the pores is equivalent for all films the linear regression for the different films would be overlapping. HPC-L shows a less linear behaviour than the other films (Figure 15) due to large variation of the permeability for the latter measure points. If these points are neglected, the linear regression is very different as can be seen in Figure 24. With that it looks like HPC-L and HPC-M are showing the same behaviour and that, if given time, would overlap. The film containing HPC-SL does not overlap with the others and this implicates that the porosity and permeability do not show the same dependency for all films containing different molecular weight HPC.

It is quite evident that the results are only approximate as the fit of the linear regression is rather poor, especially for HPC-L. These results are only presented for one replicate, and due to this insecurities can greatly affect the results and further analysis is required. The film containing the highest molecular weight HPC (HPC-M) shows a large difference in final permeability (after 26 h of exposure to water) between the permeability and the leaching experiments. This can have a great impact on the gradient of the linear regression and therefore needs to be investigated further by replicated analyses.

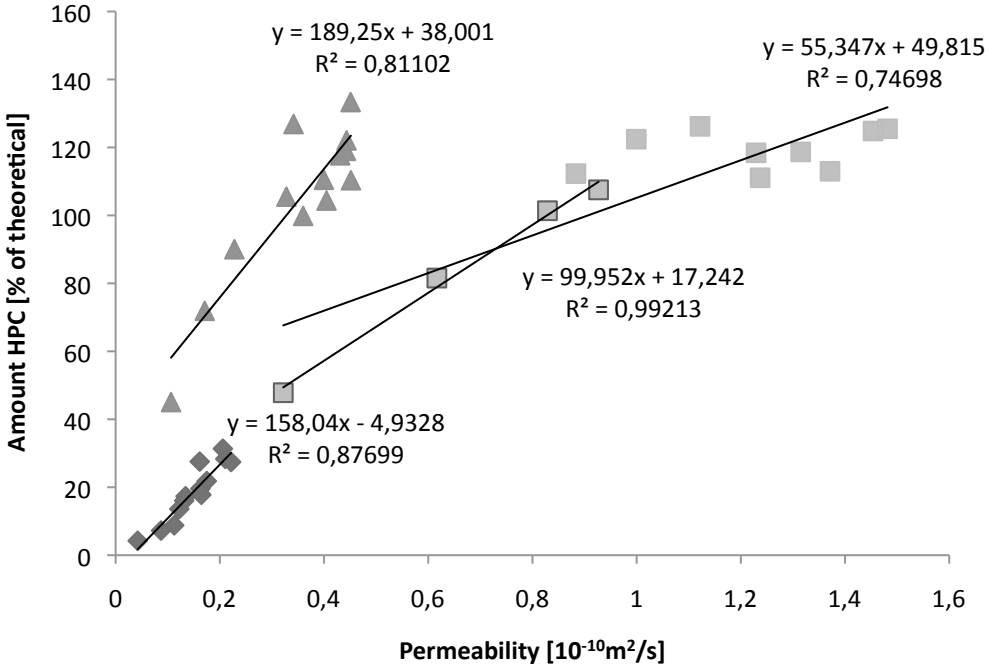

Figure 24: Graph displaying the leached amount of HPC as a function of permeability for the samples taken within 6 h from the beginning of the experiment. The linear regression for each sample series is also denoted in the graph together with the R^2 value. The graph is identical with Figure 15, but with the addition of a linear regression for the initial sample points for HPC-L. This is done to illustrate the effects of the variation in permeability for the latter sample points on the linear behaviour. ◆ HPC-M, ■ HPC-L, ▲ HPC-SL.

As mentioned earlier the lag-times before the films are fully permeable show a clear trend of increasing with increasing molecular weight of HPC (Table 8, Figure 8), which is explained by the diffusion rate of the polymers being dependent on the molecular weight. The percentage of leached HPC from the films at the determined lag-time (Table 11) is somewhere around 50% for HPC-SL and HPC-L, but only around 20% for HPC-M (HPC-SSL is not represented due to the lack of detection of this polymer). The lower value for HPC-M could be due to differences among the film pieces that were used for the permeability and leaching experiments due to differences in final permeability, as discussed earlier. The final amount of leached HPC does not show any great difference among the films, but the leaching rate might show a different

behaviour among the films. As the leaching rate was only determined for one replicate this has to be further investigated.

5.5 Structural properties and film density

A great deal of structural information of the EC10/HPC films was gained from the SEM images in Figure 16 to Figure 23. Already when examining the surfaces of the films after being exposed to water great differences in structure can be seen. Figure 16 and Figure 17 show the inner and outer surfaces of the films respectively. The outer surface, which was facing the spray nozzle in production, shows much more and smaller pores than the inner surface, which was facing the drum during production. This difference is believed to stem from the production method where the inner side dries slower than the outer side and therefore the phase separation has gone further. The differences between the different films are interesting from a molecular weight dependence point of view. The highest molecular weight HPC seems to have the smallest pore sizes, followed by the lowest molecular weight HPC. The medium molecular weights HPCs are rather similar, except for the very different structure of the inner side of HPC-L (Figure 16 h, i). Here it is almost impossible to make out individual pores and the structure seems much more continuous than that of the other films. This structure resembles the structure found on the inside of the films and it is therefore possible that this stems from the film being ripped at some point during handling to expose the inside.

When examining the pore structure of the different films (Figure 19 c to Figure 22 c) it is evident that the films exhibit different internal structures. Films containing HPC-SSL have small inclusions of HPC dispersed in the EC phase whilst films containing HPC-L have an interconnected network were it is difficult to separate each pore from each other. The distribution of pore size is very large for the low molecular weight HPC (HPC-SSL), which is an indication of phase separation according to nucleation and growth instead of spinodal decomposition. This is discussed further in chapter 5.6. The small inclusions found in EC10/HPC-M films indicate a larger EC/HPC surface area than the continuous network found in EC10/HPC-L films.

Figure 18 shows the surfaces of films that were not exposed to water. Ideally these surfaces would be homogenous and identical for all films, even though containing different molecular weight HPC. However, as can be seen in Figure 18, there are some differences in topology, which stem from variations in the production due to the film spraying method. These differences, together with other production related differences, could affect the results presented in this study as they are only from one replicate of films.

The different films show only small differences in density ranging from 1.08 to 1.11 (Table 9), but this could be a small indication of different internal structures. The film containing HPC-M has the highest density and, when examining the cross-sectional SEM image of the film not exposed to water (Figure 20 a), also show the densest structure of all the films. The film containing HPC-SSL has the lowest density and also show a much more porous structure when examining the cross-section (Figure 19 a) than the film with HPC-M. Films containing HPC-SL or HPC-L follow the same trend with internal structure and film density (Figure 21 a, Figure 22 a).

5.6 Dependence on the molecular weight of HPC on phase separation in EC/HPC mixed films

Above the properties of the different films depending on molecular weight of HPC has been discussed and various explanations for these behaviours have been presented. The EC/HPC system is a very complex system, which is far from fully understood. The dependence of the

molecular weight of HPC had previously not been examined and this study has shown significant differences in properties for films containing different molecular weight HPC. The properties which can affect the phase separation of EC and HPC are many, e.g. viscosity of the polymer solution, surface activity, phase separation mechanism etc.

5.6.1 Effect of surface tension and viscosity

The surface tension of the solutions works in favour of domain growth since the solution strives to lower the surface tension by decreasing the surface area and thereby increasing the domain size. The surface tension of an aqueous solution of HPC was determined by Chang et al to decrease with increasing concentration, especially for the low molecular weight (below 10^4) HPC [27]. Also the lower molecular weight polymers showed a slightly higher surface tension at all concentrations. Since the surface tension is highest for the lowest molecular weight HPC (HPC-SSL) this leads to the domains of this HPC being larger than the domains of the highest molecular weight HPC. This correlates with the internal structure found in the EC10/HPC-SSL and EC10/HPC-M films (Figure 19 and Figure 20). The viscosity of the solutions on the other hand, retards the growth of the domains by the polymers restricted mobility. This also works in favour of the lowest molecular weight HPC having larger domains than the highest molecular weight HPC due to the increasing viscosity.

The difference in structure and properties between the medium and high molecular weight HPC is most probably due to differences in viscosity with the highest molecular weight HPC having a much higher molecular weight than the others and therefore also have a drastically higher viscosity in concentrated solutions. The high viscosity can in this case retard the growth of the domains to such an extent that the phase separation is arrested much earlier than for the lower molecular weight HPC. This is important since the time before the film has dried and the phase separation is arrested is limited in the film spraying process.

The high molecular weight HPC investigated in this study is drastically higher than the others investigated. Due to this, it is important to be aware that for this large gap between high and medium molecular weight HPCs the trends are still unknown.

5.6.2 Effect of phase separation mechanism

Another factor that could influence the film properties and the phase separation is by which mechanism the phase separation occurs. Normally the EC/HPC solutions are said to phase separate by spinodal decomposition due to the limited parts of the phase diagram where nucleation and growth occurs. However, when examining the pore structure of the lowest molecular weight HPC (Figure 19) there is a large distribution in pore size, which is consistent with phase separation according to “nucleation and growth”. It is therefore possible that the phase separation of the lowest molecular weight HPC present in 30% occurs by a different phase separation mechanism than that of the remaining molecular weight of HPC in this study. This would explain the deviation of this film containing low molecular weight HPC compared to films with higher molecular weight HPC.

5.6.3 Bimodal molecular weight distribution

The bimodal molecular weight distribution present in the lower molecular weight HPC (Figure 5, Table 6) indicates addition of high molecular weight polymer by the manufacturer, possibly in order to increase the z-average molecular weight. The addition of a high molecular weight polymer, significantly higher as seen in Table 6, might possibly interfere with the results of this study. This since the polymer then in fact is a mixture of low and high molecular weight polymers, which, as shown e.g. in Figure 8 and Figure 10 display drastically different properties. It was not possible to determine the fractions of the different molecular weights

however, and since the fraction of the high molecular weight addition then should be smaller than possible to detect with the RI detector the influence on the results were probably, if noticeable at all, only minor.

6 Conclusion

When comparing EC/HPC mixed films containing different molecular weight HPC a presence of a maximum in permeability for EC/HPC containing 30% (w/w) HPC, which is dependent on the molecular weight of the HPC, was observed. An increase in lag-time before the film is fully permeable was seen from low molecular weight HPC to high molecular weight HPC. Beyond that, it was also shown that the molecular weight of HPC strongly influences the phase separation and the internal structure of the sprayed EC/HPC mixed films.

Together this means that even though only present in 30% the molecular weight of HPC has a great influence on the mass transport, polymer leaching and internal structure of EC/HPC mixed films. The results show that the choice of HPC in EC/HPC coatings for controlled release applications is of high importance and can be used to control the release rate of the active substance in the human body. A benefit of altering the molecular weight of HPC to control the mass transport properties of the films instead of altering the molecular weight of EC might be an alternative to avoid a decrease in mechanical properties that is occurring for low molecular weights of EC.

7 Future work

For future work within this complex system I would recommend deeper investigations regarding the phase separation mechanism and how the molecular weight of HPC affects the ternary phase diagrams for the EC/HPC solutions. Also investigation regarding the percolation limit and if this is affected by the molecular weight of HPC, is the percolation limit really the same for the high and low molecular weights as it is for the medium molecular weight HPC.

This study has shown that there are great differences within the internal structures of the films containing different molecular weight HPC. Therefore I recommend studying the diffusion of a larger substance through the film to investigate if there are any pore/solute interactions depending on molecular weight that needs to be considered when designing the controlled release coating to fit the specific application.

Indications of a difference in HPC leaching from the two sides of the films were also observed in this study and further studies within this area are recommended. This as the permeability of coated pharmaceutical pellets, where water is only present at one side, might be affected and as a result this affects the administration of the active substance.

8 References

[1] Wilson CG, Crowley, P. J. Controlled release in oral drug delivery. Rathbone MJ, editor. New York: Springer; 2011.

[2] Marucci M, Hjärtstam, J., Ragnarsson, G., Iselau, F., Axelsson, A. . Coated formulations: New insights into the release mechanism and chnages in the film properties with a novel release cell. Journal of Controlled Release. 2009;136(3):206-2012.

[3] Andersson H, Hjärtstam, J., Stading, M., von Croswant, C., Larsson, A. Effects of molecular weight on permeability and microstructure of mixed ethyl-hydroxypropyl-cellulose films. 2012.

[4] Marucci M, Ragnarsson, G., von Corswant, C., Welinder, A., Jarke, A., Iselau, F., Axelsson, A. Polymer Leaching from Film Coating: Effects on the Coating Transport Properties. International Jounal of Pharmaceutics. 2011;411(1-2):43-8.

[5] Cellulose [Encyclopedia Britannica Online] 2012 [cited 20 May. 2012]. Available from: http://www.britannica.com.proxy.lib.chalmers.se/EBchecked/topic/101633/cellulose.

[6] Viridén A. Investigation of the functionality related characteristics of hydroxypropyl methylcellulose for the release from matrix tablets. Gothenburg: Chalmers University of Technology; 2011.

[7] Lorand EJ. Cellulose Ethers - Variation of Physical Properties with Composition. Industrial and Engineering Chemistry. 1938;30(5):527-30.

[8] Holmberg K, Jönsson, B., Kronberg, B., Lindman, B. Surfactants and Polymers in Aqueous Solution. 2nd ed. Chichester: John Wiley & Sons; 2007.

[9] Hsu CC, Prausnitz, J. M. Thermodynamics of Polymer Compatibility in Ternary Systems. Macromolecules. 1974;7:320-4.

[10] Sakellariou P, Rowe, R. C., White E. F. T. Polymer/polymer interaction in blends of ethyl cellulose with both cellulose derivatives and polyethylene glycol 6000. International Jounal of Pharmaceutics. 1986;34:93-103.

[11] Permeability (physics) [Encyclopedia Britannica Online] [cited 2012-05-26]. Available from: http://www.britannica.com.

[12] Cussler EL. Diffusion - Mass Transfer in Fluid Systems. 3rd ed. Cambridge: Cambridge University Press; 2009.

[13] Cowie J, McKenzie, G., Arrighi, V. Polymers: chemistry and physics of modern materials. 3rd ed. Edinburgh: CRC Press; 2008.

[14] Strong BA. Plastics: materials and processing. Upper Saddle River: Pearson/Prentice Hall; 2006.

[15] Harris DC. Quantitative chemical analysis. 7th ed: W.H. Freeman & Company; 2006.

[16] Yeung ES, Synovec, R. R. Detectors for Liquid Chromatography. Analytical Chemistry. 1986;58(12):1237-8.

[17] Trathnigg B. Size-exclusion chromatography of polymers. In: Meyers RA, editor. Encyclopedia of Analytical Chemistry. Chichester: John Wiley & Sons Ltd; 2000. p. 8008-34.

[18] Alvarez-Lorenzo C, Duro, R., Gómez-Amoza, J. L., Martínez-Pacheco, R., Souto, C., Concheiro, A. Degradation of HydroxyPropylcellulose by *Rhizomucor*: Effects on Release from Theophylline-Hydroxypropylcellulose Tablets. International Jounal of Pharmaceutics. 1998;180:105-11.

[19] Körner A. Dissolution of polydisperse polymers in water. Lund: Lund University; 2006.

[20] Goldstein J. Scanning electron microscopy and X-ray microanalysis. New York: Kluwer Academic/Plenum Publishers; 2003.

[21] Falk CE, Posst, H. L. Liquid Scintillation Counters. American Journal of Physics. 1952;20(7):429-39.

[22] U.S.DepartmentofEnergy. DOE Handbook: Tritium handling and safe storage. In: Energy USDo, editor. Washington2008.

[23] Jarke A. Effect of manufacturing conditions and polymer ratio on the permeability and film morphology of ethyl cellulose and hydroxypropyl cellulose free-films produced using a novel spray method. Uppsala: Uppsala University; 2009.

[24] Hjärtstam J, Hjertberg, T. Studies of the Water Permeability and Mechanical Properties of a Film Made of an Ethyl Cellulose-Ethanol-Water Ternary Mixture. Journal of Applied Polymer Science. 1999;74(8):2056-62.

[25] Ye Z, Rombout, P., Remon, J. P., Vervaet, C., Van den Mooter, G. Correlation between the permeability of metoprolol tartrate through plasticized isolated ethylcellulose/hydroxypropyl methylcellulose films and drug release from reservoir pellets. European Journal of Pharmaceutics and Biopharmaceutics. 2007;67:485-90.

[26] Sakellariou P, Rowe, R. C., White E. F. T. . A Study of the LEaching/Retention of Water-Soluble Polymers in Blends with Ethylcellulose Using Torsional Braid Analysis. Journal of Controlled Release. 1988;7(2):147-57.

[27] Chang SA, Gray, D. G. The Surface Tension of Aqueous Hydroxypropyl Cellulose Solutions Journal of Colloid and Interface Science. 1978;67(2):255-65.

Appendix I

Ethyl cellulose

Viscosity grade: 10 cps
batch no: 30010001

Hydroxypropyl cellulose

HPC-SSL – batch no NAK-4511
HPC-SL – batch no NAI-0521
HPC-L – batch no NAH-0611
HPC-M – batch no NAD-0701

Appendix II

The process parameters in film spraying for the films used in this study is shown in Table 12.

Table 12: The process parameters for the films used in this study. The spray rate for the film containing HPC-M is unknown due to measurement difficulties.

	HPC-SSL	HPC-SL	HPC-L	HPC-M
Air flow (m^3/h)	40	40	40	40
Air flow temperature (°C)	72	72	72	72
Atomizer pressure (bar)	2.00	2.00	2.00	2.00
Atomizer flow (bar)	1.97	1.93	1.99	1.96
Spray rate (g/min)	14.4	14.2	14.4	12.9

Appendix III

Images of the sprayed films are presented in Figure 25 (EC10/HPC-M), Figure 26 (EC10/HPC-L), Figure 27 (EC10/HPC-SL) and Figure 28 (EC10/HPC-SSL).

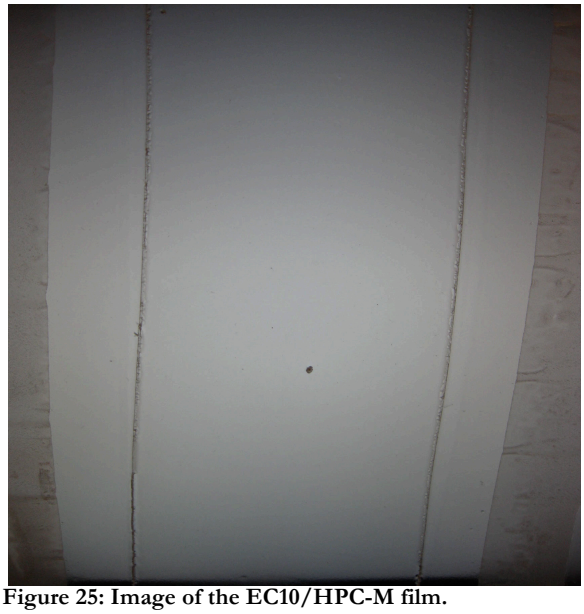

Figure 25: Image of the EC10/HPC-M film.

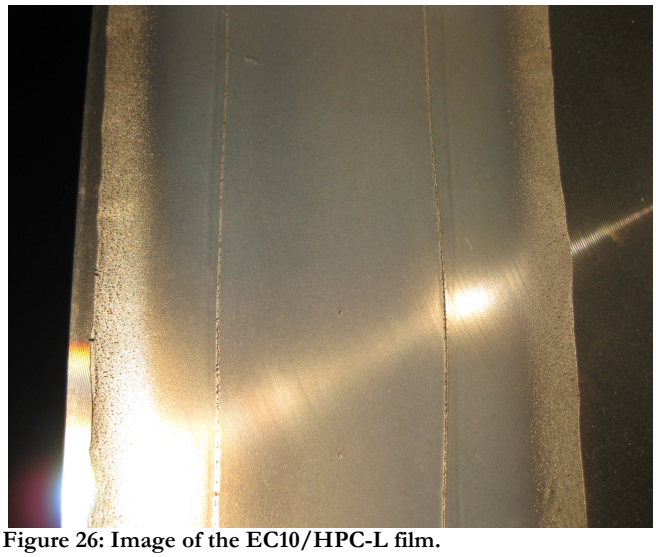

Figure 26: Image of the EC10/HPC-L film.

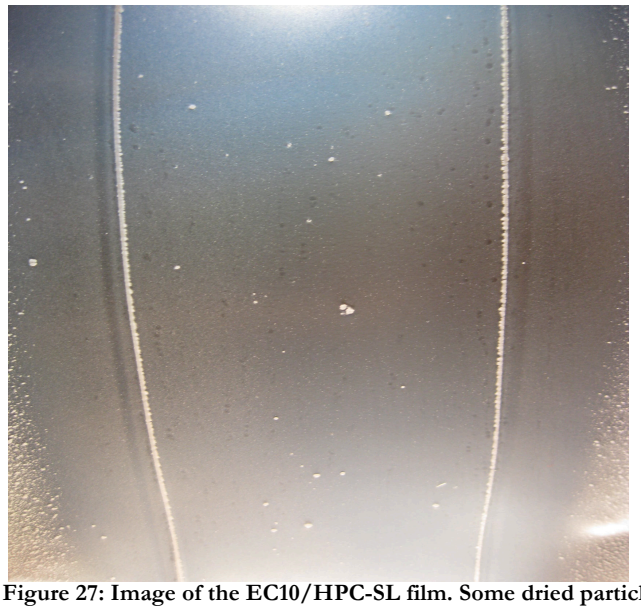

Figure 27: Image of the EC10/HPC-SL film. Some dried particles visible on the film surface.

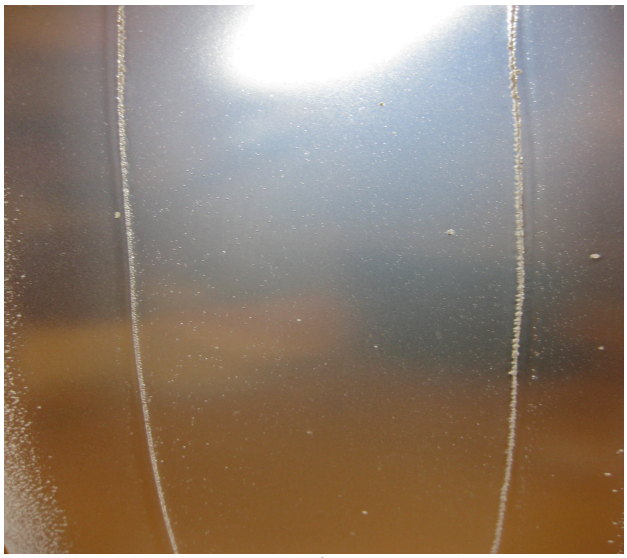

Figure 28: Image of the EC10/HPC-SSL film. Some dried particles visible on the film surface together with small bubbles.